Smart Structures and Systems, *Vol. 21, No. 1 (2018) 75-97*
DOI: https://doi.org/10.12989/sss.2018.21.1.075

Hygro-thermo-mechanical bending analysis of FGM plates using a new HSDT

Fouad Boukhelf[1], Mohamed Bachir Bouiadjra[*1,4], Mohammed Bouremana[2] and Abdelouahed Tounsi[1,2,3,4]

[1]*Laboratoire des Structures et Matériaux Avancés dans le Génie Civil et Travaux Publics (Département de Génie Civil &Travaux Publics, Faculté de Technologie, Université de Sidi Bel Abbes, Algeria*
[2]*Material and Hydrology Laboratory, University of Sidi Bel Abbes, Faculty of Technology, Civil Engineering Department, Algeria*
[3]*Department of Civil and Environmental Engineering, King Fahd University of Petroleum & Minerals, 31261 Dhahran, Eastern Province, Saudi Arabia*
[4]*Algerian National Thematic Agency of Research in Science and Technology (ATRST), Algeria*

(Received May 16, 2017, Revised December 3, 2017, Accepted December 11, 2017)

Abstract. In this paper, a novel higher-order shear deformation theory (HSDT) is proposed for the analysis of the hygro-thermo-mechanical behavior of functionally graded (FG) plates resting on elastic foundations. The developed model uses a novel kinematic by considering undetermined integral terms and only four variables are used in this model. The governing equations are deduced based on the principle of virtual work and the number of unknown functions involved is reduced to only four, which is less than the first shear deformation theory (FSDT) and others HSDTs. The Navier-type exact solutions for static analysis of simply supported FG plates subjected to hygro-thermo-mechanical loads are presented. The accuracy and efficiency of the present model is validated by comparing it with various available solutions in the literature. The influences of material properties, temperature, moisture, plate aspect ratio, side-to-thickness ratios and elastic coefficients parameters on deflections and stresses of FG plates are also investigated.

Keywords: bending; functionally graded materials; plate theory; hygro-thermo-mechanical loads

1. Introduction

Functionally graded materials (FGMs) are the novel generation of advanced composite materials in the area of engineering composites, whose characteristics are changed smoothly in the spatial direction microscopically to improve the overall structural performance. These materials provide great promise in important temperature environments, e.g., wear-resistant linings for handling large heavy abrasive ore particles, rocket heat shields, heat exchanger tubes, thermoelectric generators, heat engine components, plasma facings for fusion reactors, and electrically insulating metal/ceramic joints and also these are widely employed in many structural applications such as mechanics, civil engineering, optical, electronic, chemical, biomedical, energy sources, nuclear, automotive fields, and ship building industries to minimize thermo mechanical mismatch in metal-ceramic bonding (Reddy 2011, Yaghoobi and Yaghoobi 2013, Swaminathan and Naveenkumar 2014, Ahmed 2014, Darılmaz 2015, Kar and Panda 2015a, b, Belkorissat *et al.* 2015, Hadji and Adda Bedia 2015, Ait Yahia 2015, Akavci 2015, Bounouara *et al.* 2016, Kolahchi *et al.* 2016, Belabed *et al.* 2014, Aldousari 2017, Rahmani *et al*. 2017, Hirwani *et al*. 2018a, b, Abualnour *et al.* 2018).

Presently, various investigations are carried out for theoretically studying the thermo-mechanical response behavior of FG structures. Zhang *et al*. (1994) proposed an analytical method for FG cylinder with axial symmetry based on thermal elasticity theory. Reddy and Chen (2001) developed a three-dimensional model for a FG plate under mechanical and thermal loads, both applied at the top of the plate. The analysis of the thermo-mechanical response of hollow circular cylinders fabricated with FGM was studied by Liew *et al*. (2003). Vel and Batra (2003) presented a three-dimensional solution for transient thermal stresses in FG rectangular plates. The buckling analysis of shear deformable FG rectangular plates subjected to thermo-mechanical loads was studied by Shukla *et al*. (2007) using FSDT. The thermal bending behavior of a piezoelectric circularly curved FG actuator under an applied electric force is investigated by Zaman *et al.* (2010). Golmakani and Kadkhodayan (2011) studied a large deflection behavior of shear deformable FG plates subjected to thermo-mechanical loads and under various boundary conditions via the dynamic relaxation method. Fallah and Nosier (2012) used two parameter perturbation technique and Fourier series method to examine nonlinear response of FG circular plates with various clamped and simply supported boundary conditions. Bouderba *et al.* (2013) discussed thermo-mechanical static response of FG thick plates resting on Winkler-Pasternak elastic foundations based on a refined trigonometric shear deformation theory. Zhu *et al*. (2014)

*Corresponding author, Ph.D.
E-mail: mohamedbachirbouiadjra@gmail.com

http://www.techno-press.com/journals/sss&subpage=7
ISSN: 1738-1584 (Print), 1738-1991 (Online)

analyzed a geometrically nonlinear thermo-mechanical analysis of moderately thick FG plates by employing a local meshless method with Kriging interpolation procedure. Tung and Duc (2014) investigated the nonlinear behavior of thick FG doubly curved shallow panels resting on elastic foundations and under some conditions of mechanical, thermal, and thermo-mechanical loads. Tounsi *et al*. (2013) presented a thermo-elastic bending analysis of FG sandwich plates by employing a refined trigonometric shear deformation theory. In their work, the core layer is FGM and two face sheets have different material properties. Houari *et al*. (2013) proposed a novel higher order shear and normal deformation theory for thermo-elastic bending of FG sandwich plates. Zidi *et al*. (2014) discussed the static response of FG plates under hygro-thermo-mechanical loading using a four variable refined plate theory. Attia *et al.* (2015) presented a free vibration analysis of FG plates with temperature-dependent properties using various four variable refined plate theories. Akbaş (2015) examined the wave propagation of a functionally graded beam in thermal environments. Sobhy (2015) studied the thermo-elastic behavior of FG plates with temperature-dependent properties resting on variable elastic foundations. Mantari and Granados (2015) investigated a thermo-elastic bending behavior of two types of FGM sandwich plates by using a new quasi-3D hybrid type higher order shear deformation theory with 5 unknowns. Li *et al.* (2016) investigated the thermo-mechanical bending behavior of FG sandwich plates using four-variable refined plate theory. Laoufi *et al.* (2016) examined the mechanical and hygrothermal response of FG plates using a hyperbolic shear deformation theory. Beldjelili *et al.* (2016) studied the hygro-thermo-mechanical bending of S-FGM plates resting on variable elastic foundations using a four-variable trigonometric plate theory. Mehar and Panda (2017) presented a numerical investigation of nonlinear thermo-mechanical deflection of functionally graded CNT reinforced doubly curved composite shell panel under different mechanical loads. Recent works on flexural behavior of the composite structure using HSDT are presented by Benchohra *et al*. (2018), Youcef *et al.* (2018), Mahapatra *et al*. (2017), Abdelaziz *et al.* (2017), Chikh *et al.* (2017), Draiche *et al*. (2016), Bouafia *et al.* (2017), Benadouda *et al*. (2017, Hirwani *et al.* (2016), Bennoun *et al.* (2016), Hirwani *et al.* (2017), Bellifa *et al.* (2017a), Mahapatra *et al*. (2016a, b), Kar and Panda (2015c, 2016a,b,c), Barati and Shahverdi (2016), Barka *et al.* (2016), and Kar *et al.* (2015).

The purpose of this article is to investigate the bending response of FG plates resting on variable two-parameter elastic foundations and subjected to hygro-thermo-mechanical loads. The use of the integral term in the kinematic led to a reduction in the number of variables and equilibrium equations. These latter are deduced using the new proposed HSDT containing the hygro-thermo-mechanical effect and the interaction between the plate and the elastic foundations. The results obtained by the present theory are compared with those reported by other HSDTs available in the open literature. Some numerical examples are offered to demonstrate the influences of various parameters on the hygro-thermo-mechanical bending response of the FG plates.

2. Mathematical formulation

Consider a rectangular FG plate with sides $a \times b$ and uniform thickness h, referred to the rectangular Cartesian coordinates (x, y, z), where (x, y) plane coincides with middle surface of the plate and (z) is the thickness coordinate ($-h/2 \le z \le h/2$), as presented in Fig. 1.

The FG plate is subjected to a transverse load $q(x, y)$ and a temperature field $T(x, y, z)$ as well as a moisture concentration $C(x, y, z)$. The material characteristics of the plate are supposed to change within the thickness of the plate. By applying a simple power law distribution, the volume fractions (V) of metal and ceramic are defined as (Bessaim *et al.* 2013, Ait Amar Meziane *et al*. 2014, Bellifa *et al.* 2016, Ahouel *et al.*, 2016, Boukhari *et al.* 2016, Hanifi Hachemi Amar *et al*. 2017).

$$V_c(z) = \left(\frac{z}{h} + \frac{1}{2}\right)^p, \quad (0 \le p \le \infty), \quad V_c(z) + V_m(z) = 1 \tag{1}$$

where p is the power-law index and the subscripts c and m represent ceramic and metal, respectively. The material properties P of the FG plate, such as Young's modulus E, Poisson's ratio ν, and thermal coefficient α and moisture expansion β are expressed as (Mouffoki *et al.* 2017, El-Haina *et al*. 2017, Bouderba *et al*. 2016, Saidi *et al*. 2016, Bousahla *et al*. 2016, Hamidi *et al*. 2015, Larbi Chaht *et al*. 2015, Al-Basyouni *et al*. 2015)

$$P(z) = \left(P_c - P_m\right)V_c(z) + P_m \tag{2}$$

2.1 Displacement base field

The displacement field of the novel theory is proposed as follows (Bellifa *et al.* 2017b, Besseghier *et al*. 2017, Khetir *et al*. 2017, Menasria *et al*. 2017, Yazid *et al*. 2018, Bousahla *et al*. 2018)

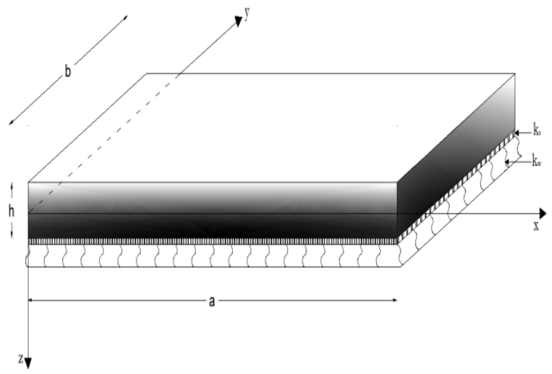

Fig. 1 Geometry and coordinates of the rectangular FG plate resting on elastic foundation

$$u(x,y,z) = u_0(x,y) - z\frac{\partial w_0}{\partial x} + k_1\, f(z)\int \theta(x,y)\,dx$$

$$v(x,y,z) = v_0(x,y) - z\frac{\partial w_0}{\partial y} + k_2\, f(z)\int \theta(x,y)\,dy \qquad \text{(3a,b,c)}$$

$$w(x,y,z) = w_0(x,y)$$

Where $u_0(x,y)$, $v_0(x,y)$, $w_0(x,y)$ and $\theta(x,y)$ are the four variable displacement functions of middle plane of the plate. The last variable is a mathematical term that allows determining the rotations of the normal to the mid plate about the x and y axes (as in the ordinary HSDT). Note that the integrals do not have limits. In the present work is considered terms with integrals instead of terms with derivatives. In this work, the present HSDT is obtained by setting

$$f(z) = \frac{z\, cosh(\pi/2) - (h/\pi) sinh\left(\frac{\pi}{h} z\right)}{cosh(\pi/2) - 1} \qquad (4)$$

It can be observed that the kinematic in Eq. (3) employs only four variables (u_0, v_0, w_0 and θ).The nonzero strains associated with the kinematic in Eq. (3) are

$$\begin{Bmatrix} \varepsilon_x \\ \varepsilon_y \\ \gamma_{xy} \end{Bmatrix} = \begin{Bmatrix} \varepsilon_x^0 \\ \varepsilon_y^0 \\ \gamma_{xy}^0 \end{Bmatrix} + z \begin{Bmatrix} k_x^0 \\ k_y^0 \\ k_{xy}^0 \end{Bmatrix} + f(z) \begin{Bmatrix} L_x^0 \\ L_y^0 \\ L_{xy}^0 \end{Bmatrix} \qquad \text{(5a)}$$

$$\begin{Bmatrix} \gamma_{yz} \\ \gamma_{xz} \end{Bmatrix} = g(z) \begin{Bmatrix} \gamma_{yz}^0 \\ \gamma_{xz}^0 \end{Bmatrix}$$

Where

$$\begin{Bmatrix} \varepsilon_x^0 \\ \varepsilon_y^0 \\ \gamma_{xy}^0 \end{Bmatrix} = \begin{Bmatrix} \dfrac{\partial u_0}{\partial x} \\ \dfrac{\partial v_0}{\partial x} \\ \dfrac{\partial u_0}{\partial y} + \dfrac{\partial v_0}{\partial x} \end{Bmatrix}, \quad \begin{Bmatrix} k_x^0 \\ k_y^0 \\ k_{xy}^0 \end{Bmatrix} = \begin{Bmatrix} -\dfrac{\partial^2 w_0}{\partial x^2} \\ -\dfrac{\partial^2 w_0}{\partial y^2} \\ -2\dfrac{\partial^2 w_0}{\partial x \partial y} \end{Bmatrix} \qquad \text{(5b)}$$

$$\begin{Bmatrix} L_x^0 \\ L_y^0 \\ L_{xy}^0 \end{Bmatrix} = \begin{Bmatrix} k_1 \theta \\ k_2 \theta \\ k_1 \dfrac{\partial}{\partial y}\int \theta\, dx + k_2 \dfrac{\partial}{\partial x}\int \theta\, dy \end{Bmatrix}$$

$$\begin{Bmatrix} \gamma_{yz}^0 \\ \gamma_{xz}^0 \end{Bmatrix} = \begin{Bmatrix} k_2 \int \theta\, dy \\ k_1 \int \theta\, dx \end{Bmatrix}$$

And

$$g(z) = \frac{df(z)}{dz} \qquad \text{(5c)}$$

The integrals used in the above equations shall be resolved by a Navier type procedure and can be expressed as follows

$$\frac{\partial}{\partial y}\int \theta\, dx = A' \frac{\partial^2 \theta}{\partial x \partial y}, \quad \frac{\partial}{\partial x}\int \theta\, dy = B' \frac{\partial^2 \theta}{\partial x \partial y}, \quad \int \theta\, dx = A' \frac{\partial \theta}{\partial x}, \quad \int \theta\, dy = B' \frac{\partial \theta}{\partial y} \qquad (6)$$

Where, the coefficients A' and B' are defined according to the type of solution employed, in this case via Navier solution. Therefore, A' , B' , k_1 and k_2 are defined as follows

$$A' = -\frac{1}{\lambda^2}, \quad B' = -\frac{1}{\mu^2}, k_1 = \lambda^2, k_2 = \mu^2 \qquad (7)$$

where λ and μ are defined in expression (24).

2.2 Constitutive equations

For the FG plate, the stress - strain relationships can be expressed as

$$\begin{Bmatrix} \sigma_x \\ \sigma_y \\ \tau_{xy} \\ \tau_{yz} \\ \tau_{xz} \end{Bmatrix} = \begin{bmatrix} C_{11} & C_{12} & 0 & 0 & 0 \\ C_{12} & C_{22} & 0 & 0 & 0 \\ 0 & 0 & C_{66} & 0 & 0 \\ 0 & 0 & 0 & C_{44} & 0 \\ 0 & 0 & 0 & 0 & C_{55} \end{bmatrix} \begin{Bmatrix} \varepsilon_x - \alpha\, \Delta T - \beta\, \Delta C \\ \varepsilon_y - \alpha\, \Delta T - \beta\, \Delta C \\ \gamma_{xy} \\ \gamma_{yz} \\ \gamma_{xz} \end{Bmatrix} \qquad (8)$$

Where (σ_x, σ_y, τ_{xy}, τ_{yz}, τ_{xz}) and (ε_x, ε_y, γ_{xy}, γ_{yz} , γ_{xz}) are the stress and strain components, respectively. Using the material properties defined in Eq. (2), stiffness coefficients, C_{ij} , can be given as

$$C_{11} = C_{22} = \frac{E(z)}{1-\nu^2}, \; C_{12} = \frac{\nu\, E(z)}{1-\nu^2}, \quad C_{44} = C_{55} = C_{66} = \frac{E(z)}{2(1+\nu)}, \qquad (9)$$

Where $\Delta T = T - T_0$ and $\Delta C = C - C_0$ in which T_0 is the reference temperature and C_0 is the reference moisture concentration. In the present work, the moisture concentration $C(x,y,z)$ and the temperature distribution field $T(x,y,z)$ are expressed as (Bouderba *et al*. 2013)

$$T(x,y,z) = T_1(x,y) + \frac{z}{h} T_2(x,y) + \overline{\Psi}(z) T_2(x,y) \qquad \text{(10a)}$$

$$C(x,y,z) = C_1(x,y) + \frac{z}{h} C_2(x,y) + \overline{\Psi}(z) C_2(x,y) \qquad \text{(10b)}$$

In which $\overline{\Psi}(z)=\frac{1}{\pi}\sin\left(\frac{\pi}{h}z\right)$ in the case of sinusoidal temperature distribution, $\overline{\Psi}(z)=\frac{z}{h}\left(1-\frac{4}{3}\left(\frac{z}{h}\right)^2\right)$ in the case of cubic temperature distribution and $\overline{\Psi}(z)=\frac{z}{h}e^{-2\left(\frac{z}{h}\right)^2}$ in the case of exponential temperature distribution.

2.3 Governing equations

The governing equations of equilibrium can be determined by using the principle of virtual displacements. The principle of virtual work in the this case yields (Zidi *et al*. 2017, Houari *et al.* 2016, Bousahla *et al.* 2014, Hebali *et al*. 2014, Bourada *et al*. 2015, Mahi *et al*. 2015, Zemri *et al.* 2015)

$$\begin{aligned}&\int_{\Omega}\int_{-h/2}^{h/2}\left[\sigma_x\,\delta\,\varepsilon_x+\sigma_y\,\delta\,\varepsilon_y+\tau_{xy}\,\delta\,\gamma_{xy}+\tau_{xz}\,\delta\,\gamma_{xz}+\tau_{yz}\,\delta\,\gamma_{yz}\right]d\,z\,d\,\Omega\\&-\int_{\Omega}(q-f_e)\delta\,w\;d\,\Omega=0\end{aligned}\tag{11}$$

Where Ω is the top surface, and f_e is the density of reaction force of foundation. For the Pasternak foundation model

$$f_e=K_w w-K_{sx}\frac{\partial^2 w}{\partial x^2}-K_{sy}\frac{\partial^2 w}{\partial y^2}\tag{12}$$

where K_w is the modulus of subgrade reaction (elastic coefficient of the foundation) and K_{sx} and K_{sy} are the shear moduli of the subgrade (shear layer foundation stiffness). If the foundation is homogeneous and isotropic, this implies that $K_{sx}=K_{sy}=K_s$. If the shear layer foundation stiffness is neglected, Pasternak foundation becomes a Winkler foundation.

Substituting Eqs. (5) and (8) into Eq. (12) and integrating across the thickness of the plate, Eq. (12) can be expressed as

$$\begin{aligned}&\int_{\Omega}\Big[N_x\delta\,\varepsilon_x^0+N_y\delta\,\varepsilon_y^0+N_{xy}\delta\,\gamma_{xy}^0+M_x\delta\,k_x^0+M_y\delta\,k_y^0+M_{xy}\delta\,k_{xy}^0\\&\quad+S_x\delta\,L_x^0+S_y\delta\,L_y^0+S_{xy}\delta\,L_{xy}^0+R_{yz}\delta\,\gamma_{yz}^0+R_{xz}\delta\,\gamma_{xz}^0\Big]d\Omega-\int_{\Omega}(q-f_e)\delta\,w\,d\,\Omega=0\end{aligned}\tag{13}$$

where the stress resultants N , M , S , and R are defined by

$$\begin{aligned}&(N_i,M_i,S_i)=\int_{-h/2}^{h/2}(1,z,f)\sigma_i\;d\;z\,,\quad(i=x,y,xy)\text{ and}\\&(R_{xz},R_{yz})=\int_{-h/2}^{h/2}g\left(\tau_{xz},\tau_{yz}\right)d\;z\end{aligned}\tag{14}$$

Substituting Eq. (8) into Eq. (15) and integrating across the thickness of the plate, the stress resultants are expressed as

$$\begin{Bmatrix}N_x\\N_y\\N_{xy}\\M_x\\M_y\\M_{xy}\\S_x\\S_y\\S_{xy}\end{Bmatrix}=\begin{bmatrix}A_{11}&A_{12}&0&B_{11}&B_{12}&0&B_{11}^s&B_{12}^s&0\\A_{12}&A_{22}&0&B_{12}&B_{22}&0&B_{12}^s&B_{22}^s&0\\0&0&A_{66}&0&0&B_{66}&0&0&B_{66}^s\\B_{11}&B_{12}&0&D_{11}&D_{12}&0&D_{11}^s&D_{12}^s&0\\B_{12}&B_{22}&0&D_{12}&D_{22}&0&D_{12}^s&D_{22}^s&0\\0&0&B_{66}&0&0&D_{66}&0&0&D_{66}^s\\B_{11}^s&B_{12}^s&0&D_{11}^s&D_{12}^s&0&H_{11}^s&H_{12}^s&0\\B_{12}^s&B_{22}^s&0&D_{12}^s&D_{22}^s&0&H_{12}^s&H_{22}^s&0\\0&0&B_{66}^s&0&0&D_{66}^s&0&0&H_{66}^s\end{bmatrix}\begin{Bmatrix}\varepsilon_x^0\\\varepsilon_y^0\\\gamma_{xy}^0\\k_x^0\\k_y^0\\k_{xy}^0\\L_x^0\\L_y^0\\L_{xy}^0\end{Bmatrix}-\begin{Bmatrix}N_x^T\\N_y^T\\0\\M_x^T\\M_y^T\\0\\S_x^T\\S_y^T\\0\end{Bmatrix}-\begin{Bmatrix}N_x^C\\N_y^C\\0\\M_x^C\\M_y^C\\0\\S_x^C\\S_y^C\\0\end{Bmatrix}\tag{15a}$$

$$\begin{Bmatrix}R_{yz}\\R_{xz}\end{Bmatrix}=\begin{bmatrix}A_{44}^s&0\\0&A_{55}^s\end{bmatrix}\begin{Bmatrix}\gamma_{yz}^0\\\gamma_{xz}^0\end{Bmatrix}\tag{15b}$$

Where stiffness components are defined as

$$\begin{Bmatrix}A_{11}&B_{11}&D_{11}&B_{11}^s&D_{11}^s&H_{11}^s\\A_{12}&B_{12}&D_{12}&B_{12}^s&D_{12}^s&H_{12}^s\\A_{66}&B_{66}&D_{66}&B_{66}^s&D_{66}^s&H_{66}^s\end{Bmatrix}=\int_{-h/2}^{h/2}C_{11}\left(1,z,z^2,f(z),z\,f(z),f^2(z)\right)\begin{Bmatrix}1\\\nu\\\frac{1-\nu}{2}\end{Bmatrix}dz\tag{16a}$$

$$\left(A_{22},B_{22},D_{22},B_{22}^s,D_{22}^s,H_{22}^s\right)=\left(A_{11},B_{11},D_{11},B_{11}^s,D_{11}^s,H_{11}^s\right)\tag{16b}$$

The stress and moment resultants, $N_x^T=N_y^T$, $M_x^T=M_y^T$, $S_x^T=S_y^T$, $N_x^C=N_y^C$, $M_x^C=M_y^C$, $S_x^C=S_y^C$, to thermal and hygroscopic loading are defined by

$$\begin{Bmatrix}N_x^T\\M_x^T\\S_x^T\end{Bmatrix}=\int_{-h/2}^{h/2}\frac{E(z)}{1-\nu}\alpha(z)T\begin{Bmatrix}1\\z\\f(z)\end{Bmatrix}dz\tag{17a}$$

$$\begin{Bmatrix}N_x^C\\M_x^C\\S_x^C\end{Bmatrix}=\int_{-h/2}^{h/2}\frac{E(z)}{1-\nu}\beta(z)C\begin{Bmatrix}1\\z\\f(z)\end{Bmatrix}dz\tag{17b}$$

The governing equations of equilibrium can be obtained from Eq. (14) by integrating the displacement gradients by parts and setting the coefficients δu_0 , δv_0 , δw_0 and $\delta\theta$ zero separately. Thus one can obtain the governing equations associated with the present HSDT

$$
\begin{aligned}
&\delta\, u_0: \quad \frac{\partial N_x}{\partial x}+\frac{\partial N_{xy}}{\partial y}=0 \\
&\delta\, v_0: \quad \frac{\partial N_{xy}}{\partial x}+\frac{\partial N_y}{\partial y}=0 \\
&\delta\, w_0: \quad \frac{\partial^2 M_x}{\partial x^2}+2\frac{\partial^2 M_{xy}}{\partial x \partial y}+\frac{\partial^2 M_y}{\partial y^2}+f_e+q=0 \\
&\delta\, \theta: \quad -k_1 S_x - k_2 S_y - k_1 \frac{\partial^2 S_{xy}}{\partial x \partial y} A' - k_2 \frac{\partial^2 S_{xy}}{\partial x \partial y} B' + k_1 A' \frac{\partial R_{xz}}{\partial x} + k_2 B' \frac{\partial R_{yz}}{\partial y} = 0
\end{aligned} \tag{18}
$$

By substituting Eq. (16) into Eq. (19), the governing equations can be expressed in terms of generalized displacements as

$$
\begin{aligned}
&A_{11} d_{11} u_0 + A_{66} d_{22} u_0 + \left(A_{12}+A_{66}\right) d_{12} v_0 - B_{11} d_{111} w_0 - \left(B_{12}+2B_{66}\right) d_{122} w_0 \\
&+\left(B_{66}^s \left(k_1 A' + k_2 B'\right) + B_{12}^s k_2 B'\right) d_{122}\theta + B_{11}^s k_1 A' d_{111}\theta = F_1
\end{aligned} \tag{19a}
$$

$$
\begin{aligned}
&A_{22} d_{22} v_0 + A_{66} d_{11} v_0 + \left(A_{12}+A_{66}\right) d_{12} u_0 - B_{22} d_{222} w_0 - \left(B_{12}+2B_{66}\right) d_{112} w_0 \\
&+\left(B_{66}^s \left(k_1 A' + k_2 B'\right) + B_{12}^s k_1 A'\right) d_{112}\theta + B_{22}^s k_2 B' d_{222}\theta = F_2
\end{aligned} \tag{19b}
$$

$$
\begin{aligned}
&B_{11} d_{111} u_0 + \left(B_{12}+2B_{66}\right) d_{122} u_0 + \left(B_{12}+2B_{66}\right) d_{112} v_0 + B_{22} d_{222} v_0 - D_{11} d_{1111} w_0 - 2\left(D_{12}+2D_{66}\right) d_{1122} w_0 \\
&-D_{22} d_{2222} w_0 + D_{11}^s k_1 A' d_{1111}\theta \\
&+\left(\left(D_{12}^s+2D_{66}^s\right)\left(k_1 A' + k_2 B'\right)\right) d_{1122}\theta + D_{22}^s k_2 B' d_{2222}\theta + f_e = F_3
\end{aligned} \tag{19c}
$$

$$
\begin{aligned}
&-k_1 A' B_{11}^s d_{111} u_0 - \left(B_{12}^s k_2 B' + B_{66}^s \left(k_1 A' + k_2 B'\right)\right) d_{122} u_0 - \left(B_{12}^s k_1 A' + B_{66}^s \left(k_1 A' + k_2 B'\right)\right) d_{112} v_0 - B_{22}^s k_2 B' d_{222} v_0 \\
&+D_{11}^s k_1 A' d_{1111} w_0 + \left(\left(D_{12}^s + 2D_{66}^s\right)\left(k_1 A' + k_2 B'\right)\right) d_{1122} w_0 + D_{22}^s k_2 B' d_{2222} w_0 - H_{11}^s \left(k_1 A'\right)^2 d_{1111}\theta \\
&-H_{22}^s \left(k_2 B'\right)^2 d_{2222}\theta - \left(2H_{12}^s k_1 k_2 A' B' + \left(k_1 A' + k_2 B'\right)^2 H_{66}^s\right) d_{1122}\theta + A_{44}^s k_1 A'^2 d_{11}\theta + A_{55}^s k_2 B'^2 d_{22}\theta = F_4
\end{aligned} \tag{19d}
$$

Where d_{ij} , d_{ijl} and d_{ijlm} are the following differential operators

$$
\begin{aligned}
&d_{ij} = \frac{\partial^2}{\partial x_i \partial x_j}, \quad d_{ijl} = \frac{\partial^3}{\partial x_i \partial x_j \partial x_l}, \\
&d_{ijlm} = \frac{\partial^4}{\partial x_i \partial x_j \partial x_l \partial x_m}, \quad d_i = \frac{\partial}{\partial x_i}, \\
&(i, j, l, m = 1,2).
\end{aligned} \tag{20}
$$

where $\{F\} = \{F_1, F_2, F_3, F_4\}^t$ is generalized force vector.

The components of the generalized force vector $\{F\}$ are given by

$$
F_1 = \frac{\partial N_x^T}{\partial x} + \frac{\partial N_x^C}{\partial x}, \quad F_2 = \frac{\partial N_y^T}{\partial y} + \frac{\partial N_y^C}{\partial y}, \tag{21}
$$

$$
\begin{aligned}
&F_3 = -q + \frac{\partial^2 \left(M_x^T + M_x^C\right)}{\partial x^2} + \frac{\partial^2 \left(M_y^T + M_y^C\right)}{\partial y^2}, \\
&F_4 = \frac{\partial^2 \left(S_x^T + S_x^C\right)}{\partial x^2} + \frac{\partial^2 \left(S_y^T + S_y^C\right)}{\partial y^2}
\end{aligned}
$$

3. Analytical solution for simply-supported FG plates

Rectangular plates are generally classified in accordance with the type of support employed. We are here concerned with the exact solution of Eqs. (20) for a simply supported FG plate. To solve this problem, Navier supposed that the transverse mechanical, temperature and moisture loads, q , T_i and C_i in the form of a in the double Fourier series as

$$
\begin{Bmatrix} q \\ T_i \\ C_i \end{Bmatrix} = \begin{Bmatrix} q_0 \\ t_i \\ c_i \end{Bmatrix} \sin(\lambda\, x)\sin(\mu\, y), \quad (i = 1,2,3) \tag{22}
$$

where q_0, t_i and c_i are constants and T_i and C_i are defined in Eq. (11). with

$$
\lambda = m\pi / a \quad \text{and} \quad \mu = n\pi / b \tag{23}
$$

Following the Navier method, we consider the following solution form for u_0, v_0, w_0 and θ that satisfies the boundary conditions

$$
\begin{Bmatrix} u_0 \\ v_0 \\ w_0 \\ \theta \end{Bmatrix} = \begin{Bmatrix} U \cos(\lambda\, x)\sin(\mu\, y) \\ V \sin(\lambda\, x)\cos(\mu\, y) \\ W \sin(\lambda\, x)\sin(\mu\, y) \\ X \sin(\lambda\, x)\sin(\mu\, y) \end{Bmatrix} \tag{24}
$$

where U , V , W , and X are arbitrary parameters to be determined subjected to the condition that the solution in Eq. (25) satisfies governing Eq. (20). Substituting Eq. (25) intoEqs. (20), one obtains

$$
\begin{bmatrix} S_{11} & S_{12} & S_{13} & S_{14} \\ S_{12} & S_{22} & S_{23} & S_{24} \\ S_{13} & S_{23} & S_{33} & S_{34} \\ S_{14} & S_{24} & S_{34} & S_{44} \end{bmatrix} \begin{Bmatrix} U \\ V \\ W \\ X \end{Bmatrix} = \begin{Bmatrix} F_1 \\ F_2 \\ F_3 \\ F_4 \end{Bmatrix} \tag{25}
$$

Where

$$
\begin{aligned}
&S_{11} = -A_{11}\lambda^2 - A_{66}\mu^2, \quad S_{12} = -\lambda\mu\left(A_{12}+A_{66}\right), \\
&S_{13} = \lambda\left(B_{11}\lambda^2 + (B_{12}+2B_{66})\mu^2\right),
\end{aligned} \tag{26}
$$

$$
S_{14} = -\lambda\left(\left(k_2 B' B_{12}^s + \left(k_1 A' + k_2 B'\right) B_{66}^s\right)\mu^2 + k_1 A' B_{11}^s \lambda^2\right)
$$

$$
\begin{aligned}
&S_{22} = -A_{66}\lambda^2 - A_{22}\mu^2, \\
&S_{23} = \mu\left(B_{22}\mu^2 + (B_{12}+2B_{66})\lambda^2\right),
\end{aligned}
$$

$$S_{24} = -\mu\left((k_1 A' B_{12}^s + \left(k_1 A' + k_2 B'\right) B_{66}^s)\lambda^2 + k_2 B' B_{22}^s \mu^2\right),$$
$$S_{33} = \lambda^2\mu^2\left(D_{11}k_1B'\lambda^2 + (D_{12} + 2D_{66})(k_1A' + k_2B') + D_{22}k_2A'\mu^2 - K_w(A'B') + K_{sx}B' + K_{sy}A'\right)$$
$$S_{34} = k_1 A' D_{11}^s \lambda^4 + ((D_{12}^s + 2D_{66}^s)(k_1A' + k_2B'))\lambda^2\mu^2 + k_2 B' D_{22}^s \mu^4$$
$$S_{44} = -(k_1A')^2 H_{11}^s\lambda^4 - (2k_1k_2A'B'H_{12}^s + (k_1A' + k_2B')^2 H_{66}^s)\lambda^2\mu^2 - (k_2B')^2 H_{22}^s\mu^4$$
$$-\left(k_1A'\right)^2 A_{44}^s\lambda^2 - \left(k_2B'\right)^2 A_{55}^s\mu^2$$

The components of the generalized force vector $\{F\} = \{F_1, F_2, F_3, F_4\}^t$ are given by

$$F_1 = \lambda\left(A^T t_1 + B^T t_2 + {}^aB^T t_3 + A^C c_1 + B^C c_2 + {}^aB^C c_3\right) \tag{27a}$$

$$F_2 = \mu\left(A^T t_1 + B^T t_2 + {}^aB^T t_3 + A^C c_1 + B^C c_2 + {}^aB^C c_3\right) \tag{27b}$$

$$F_3 = -q_0 - h\left(\lambda^2 + \mu^2\right)\left(B^T t_1 + D^T t_2 + {}^aD^T t_3 + B^C c_1 + D^C c_2 + {}^aD^C c_3\right) \tag{27c}$$

$$F_4 = -h\left(\lambda^2 + \mu^2\right)\left({}^sB^T t_1 + {}^sD^T t_2 + {}^sF^T t_3 + {}^sB^C c_1 + {}^sD^C c_2 + {}^sF^C c_3\right) \tag{27d}$$

Where

$$\left[A^T, B^T, D^T\right] = \int_{-h/2}^{h/2} \frac{E(z)}{1-\nu}\alpha(z)\left[1, \bar{z}, \bar{z}^2\right]dz \tag{28a}$$

$$\left[A^C, B^C, D^C\right] = \int_{-h/2}^{h/2} \frac{E(z)}{1-\nu}\beta(z)\left[1, \bar{z}, \bar{z}^2\right]dz \tag{28b}$$

$$\left[{}^aB^T, {}^aD^T\right] = \int_{-h/2}^{h/2} \frac{E(z)}{1-\nu}\alpha(z)\bar{\Psi}(z)\left[1, \bar{z}\right]dz \tag{28c}$$

$$\left[{}^aB^C, {}^aD^C\right] = \int_{-h/2}^{h/2} \frac{E(z)}{1-\nu}\beta(z)\bar{\Psi}(z)\left[1, \bar{z}\right]dz \tag{28d}$$

$$\left[{}^sB^T, {}^sD^T, {}^sF^T\right] = \int_{-h/2}^{h/2} \frac{E(z)}{1-\nu}\alpha(z)\bar{f}(z)\left[1, \bar{z}, \bar{\Psi}(z)\right]dz \tag{28e}$$

$$\left[{}^sB^C, {}^sD^C, {}^sF^C\right] = \int_{-h/2}^{h/2} \frac{E(z)}{1-\nu}\beta(z)\bar{f}(z)\left[1, \bar{z}, \bar{\Psi}(z)\right]dz \tag{28f}$$

In which $\bar{z} = z/h$ and $\bar{f}(z) = f(z)/h$.

4. Analytical solution for simply-supported FG plates

In this section, numerical examples are proposed and discussed for checking the accuracy of the developed new theory in investigating the hygro-thermo-mechanical bending behaviours of plates. Comparisons are carried out with available solutions in literature. In order to verify the accuracy of the present analysis, some numerical examples are solved. The obtained results are compared with those of other shear deformation theories available in literature such as Laoufi *et al.* (2016), third shear deformation theory (TSDT) and sinusoidal shear deformation theory (SSDT) of Zenkour (2006). The material properties of the FGM are reported in Table 1.

In this work, the numerical results for the mechanical loading is shown in the dimensionless quantities defined as follows

$$\bar{w} = \frac{10h^3E_c}{a^4q_0}w\left(\frac{a}{2},\frac{b}{2}\right), \bar{\sigma}_x = \frac{h}{aq_0}\sigma_x\left(\frac{a}{2},\frac{b}{2},\frac{h}{2}\right),$$
$$\bar{\tau}_{xy} = \frac{h}{aq_0}\tau_{xy}\left(0,0,\frac{-h}{3}\right), \bar{\tau}_{xz} = \frac{h}{aq_0}\tau_{xz}\left(0,\frac{b}{2},0\right) \tag{29}$$
$$, k_w = \frac{K_w a^4}{D}, \quad k_s = \frac{K_s a^2}{D}, \quad D = \frac{Eh^3}{12\left(1-\nu?\right)}$$

Tables 2 and 3 list the non-dimensional transverse and stresses of a FG square plate with side-to-thickness ratio $a/h = 10$. It can be shown from these tables that results predicted by the proposed HSDT are in an excellent agreement with those obtained using SSDT (Zenkour 2006), of Laoufi *et al.* (2016) and TSDT (Reddy 2000).

In the second examples, a comparison study is presented and discussed for checking the accuracy of the proposed theory in investigating the bending behavior of FG plates under sinusoidal load and a temperature field $T(x,y,z)$ as well as moisture concentration $C(x,y,z)$. The material characteristics are considered in the investigation at the reference temperature $T_0 = 25$ °C (room temperature) and moisture concentration $C_0 = 0\%$ as shown in Table 4.

In the following, the non-dimensional quantities are defined as

$$\bar{w} = \frac{10^2 D}{a^4 q_0}w\left(\frac{a}{2},\frac{b}{2}\right),$$
$$\bar{\sigma}_x = \frac{1}{10^2 q_0}\sigma_x\left(\frac{a}{2},\frac{b}{2},\frac{h}{2}\right), \tag{30}$$
$$\bar{\tau}_{xy} = \frac{1}{10q_0}\tau_{xy}\left(0,0,\frac{-h}{3}\right), \bar{\tau}_{xz} = -\frac{1}{10q_0}\tau_{xz}\left(0,\frac{b}{2},0\right),$$
$$k_w = \frac{K_w a^4}{D}, \quad k_s = \frac{K_s a^2}{D}, \quad D = \frac{Eh^3}{12\left(1-\nu?\right)}$$

Table 1 Material properties used in the FG plate

Properties	Metal, Ti-6Al-4V	Ceramic Zerconia, ZrO_2
E (GPa)	70	380
ν	0.3	0.3

Table 2 Effects of volume fraction exponent on the dimensionless displacements and stresses of a FG square plate ($a/h=10$, $k_w=k_s=0$, $q_0=1$, $T=C=0$)

p	Theory	$\bar{w}$	$\bar{\sigma}_x$	$\bar{\tau}_{xy}$	$\bar{\tau}_{xz}$
Ceramic	Present	0.29597	1.99322	0.70682	0.23101
	TSDT(Reddy 2000)	0.294	1.98915	0.70557	0.23778
	Zankour (2006)	0.296	1.9955	0.7065	0.2462
	Laoufi *et al.* (2015)	0.29604	2.02724	0.70678	0.23215
1	Present	0.588799	3.08315	0.611186	0.23101
	TSDT(Reddy 2000)	0.58895	3.08501	0.61111	0.23817
	Zankour (2006)	0.5889	3.087	0.611	0.2462
	Laoufi *et al.* (2015)	0.58893	3.12645	0.61118	0.23215
2	Present	0.75696	3.60419	0.54433	0.21066
	TSDT(Reddy 2000)	0.75747	3.60664	0.54434	0.22568
	Zankour (2006)	0.7573	3.6094	0.5441	0.2265
	Laoufi *et al*. (2015)	0.75718	3.63002	0.54432	0.2119
3	Present	0.83687	3.86769	0.55281	0.19413
	Zankour (2006)	0.8377	3.8742	0.5525	0.2107
	Laoufi *et al.* (2015)	0.83717	3.86808	0.55278	0.19543
4	Present	0.88065	4.06191	0.56713	0.18592
	Zankour (2006)	0.8819	4.0693	0.5667	0.2029
	Laoufi *et al*. (2015)	0.88102	4.03991	0.5671	0.18728
5	Present	0.91037	4.24082	0.57586	0.18434
	TSDT(Reddy 2000)	0.90951	4.24293	0.57368	0.21609
	Zankour (2006)	0.9118	4.2488	0.5755	0.2017
	Laoufi *et al*. (2015)	0.9108	4.20242	0.57585	0.18575
6	Present	0.934029	4.41601	0.580769	0.186597
	Zankour (2006)	0.9356	4.4244	0.5803	0.2041
	Laoufi *et al*. (2015)	0.93452	4.36696	0.58075	0.18807
7	Present	0.954678	4.58872	0.583804	0.190548
	Zankour (2006)	0.9562	4.5971	0.5834	0.2081
	Laoufi *et al.* (2015)	0.95521	4.53333	0.58378	0.19206
8	Present	0.973533	4.7577	0.586039	0.194901
	Zankour (2006)	0.975	4.7661	0.5856	0.2124
	Laoufi *et al*. (2015)	0.97408	4.69925	0.58602	0.19645
9	Present	0.99115	4.92201	0.58796	0.19902
	Zankour (2006)	0.9925	4.9303	0.5875	0.2164
	Laoufi *et al*. (2015)	0.9917	4.86294	0.58794	0.20059
10	Present	1.00775	5.08083	0.58981	0.20265
	Zankour (2006)	1.0089	5.089	0.5894	0.2198
	Laoufi *et al.* (2015)	1.00832	5.02282	0.58977	0.20424
Metal	Present	1.60667	1.99322	0.70682	0.23101
	TSDT(Reddy, 2000)	1.59724	1.98915	0.70557	0.23778
	Zankour (2006)	1.607	1.9955	0.7065	0.2462
	Laoufi *et al*. (2015)	1.57882	1.89911	0.70234	0.24229

Table 3 Effects of volume fraction exponent and elastic foundation parameters on the dimensionless displacements and stresses of a FGM rectangular plate (a/h = 10, b = 3a, q_0 = 100, t_1 = t_3 = 0, t_2 = 10, c_1 = c_3 = 0, c_2 = 100)

p	k_w	k_s	Theory	$\bar{w}$	$\bar{\sigma}_x$	$\bar{\tau}_{xy}$	$\bar{\tau}_{xz}$
Ceramic	0	0	Present	0.29597	1.99322	0.70682	0.23101
			Present	1.80647	0.47165	1.55994	-0.408538
			Laoufi *et al.* (2015)	1.80709	0.46227	1.5599	-0.41798
			TSDT	1.80712	0.47187	1.55982	-0.42955
	100	0	SSDT	1.80708	0.472	1.55975	-0.44327
			Present	0.972134	-0.027288	0.852158	-0.011384
			Laoufi *et al.* (2015)	0.97215	-0.02729	0.85215	-0.01164
			TSDT	0.97216	-0.0274	0.85211	-0.01197
	0	100	Present	0.188661	-0.495817	0.187525	0.361559
			Laoufi *et al.* (2015)	0.1886	-0.48723	0.18797	0.36968
			TSDT	0.18861	-0.4957	0.18806	0.3799
			SSDT	0.18861	-0.49588	0.1881	0.39206
	100	100	Present	0.173143	-0.505098	0.17436	0.368946
			Laoufi *et al.* (2015)	0.17309	-0.49633	0.17482	0.37723
			TSDT	0.17309	-0.50498	0.1749	0.38766
			SSDT	0.17309	-0.50716	0.17495	0.40007
0.5	100	100	Present	0.18416	-0.519873	0.182428	0.422388
			Laoufi *et al.* (2015)	0.18409	-0.50982	0.18292	0.43981
			TSDT	0.1841	-0.51975	0.18299	0.44334
			SSDT	0.18411	-0.51999	0.18301	0.45728
1	100	100	Present	0.185098	-0.514645	0.155729	0.42383
			Laoufi *et al.* (2015)	0.18503	-0.50181	0.15622	0.4334
			TSDT	0.18504	-0.5145	0.15631	0.44545
			SSDT	0.18504	-0.51476	0.15635	0.45984
2	100	100	Present	0.185664	-0.503584	0.133831	0.415814
			Laoufi *et al.* (2015)	0.18559	-0.48892	0.13438	0.42571
			TSDT	0.1856	-0.50336	0.13451	0.43831
			SSDT	0.1856	-0.50363	0.13461	0.45337
5	100	100	Present	0.187038	-0.489732	0.123353	0.414022
			Laoufi *et al.* (2015)	0.18696	-0.47268	0.1234	0.42443
			TSDT	0.19696	-0.4894	0.12417	0.43754
			SSDT	0.18694	-0.48967	0.12431	0.45322
Metal	100	100	Present	0.188464	-0.594955	0.120202	0.437745
			Laoufi *et al.* (2015)	0.18842	-0.4228	0.12011	0.4468
			TSDT	0.1884	-0.43095	0.12087	0.45993
			SSDT	0.1884	-0.43117	0.12092	0.47465

Table 4 Material properties used in the FG plate

Properties	Metal (Ti-6Al-4V)	Ceramic Zerconia,(ZrO_2)
E (GPa)	66.2	117
ν	1/3	1/3
$\alpha\left(10^{-6}/C^0\right)$	10.3	7.11
$\beta\left(10^{-6}/K^0\right)$	0.33	0

Table 5 Effects of volume fraction exponent and elastic foundation parameters on the dimensionless displacements and stresses of a FG rectangular plate (a/h = 10, b = 3a, $q0$ = 100, $t1$ = 0, $t2$ = $t3$ = 10, $c1$ = 0, $c2$ = $c3$ = 100)

p	k_w	k_p	Theory	$\bar{w}$	$\bar{\sigma}_x$	$\bar{\tau}_{xy}$	$\bar{\tau}_{xz}$
Ceramic	0	0	Present	2.54014	0.525163	2.20384	-0.404199
			Laoufi *et al*. (2015)	2.54076	0.51588	2.20381	-0.41354
			TSDT	2.54076	0.52522	2.20374	-0.42454
			SSDT	2.54068	0.52552	2.20366	-0.43753
	100	0	Present	1.36695	-0.176414	1.20861	0.154253
			Laoufi *et al*. (2015)	1.36683	-0.17281	1.20872	0.15777
			TSDT	1.36682	-0.17643	1.20877	0.16257
			SSDT	1.3668	-0.17649	1.20881	0.16834
	0	100	Present	0.265285	-0.835229	0.274052	0.678662
			Laoufi *et al*. (2015)	0.26517	-0.8191	0.27488	0.6939
			TSDT	0.26518	-0.835	0.27507	0.71354
			SSDT	0.26518	-0.83531	0.27519	0.73692
	100	100	Present	0.243462	-0.848278	0.25554	0.689049
			Laoufi *et al*. (2015)	0.24336	-0.8319	0.25639	0.70452
			TSDT	0.24336	-0.84804	0.25658	0.72442
			SSDT	0.24337	-0.84835	0.2567	0.74816
0.5	100	100	Present	0.262064	-0.872634	0.279282	0.780308
			Laoufi *et al*. (2015)	0.26194	-0.86236	0.28023	0.75161
			TSDT	0.26195	-0.87239	0.28034	0.81947
			SSDT	0.26196	-0.87282	0.28041	0.84586
1	100	100	Present	0.263417	-0.862338	0.236503	0.781178
			Laoufi *et al*. (2015)	0.2633	-0.83867	0.23741	0.79871
			TSDT	0.2633	-0.86205	0.23762	0.82148
			SSDT	0.2633	-0.86252	0.23772	0.84866
2	100	100	Present	0.264093	-0.841791	0.200059	0.764692
			Laoufi *et al*. (2015)	0.26396	-0.81483	0.20107	0.78289
			TSDT	0.26396	-0.84138	0.20133	0.80652
			SSDT	0.26395	-0.84185	0.20154	0.83484
5	100	100	Present	0.266174	-0.818065	0.183053	0.759403
			Laoufi *et al*. (2015)	0.26603	-0.78678	0.18423	0.77849
			TSDT	0.26601	-0.81745	0.18459	0.80297
			SSDT	0.266	-0.81792	0.18486	0.8323
Metal	100	100	Present	0.267874	-0.985018	0.181616	0.799027
			Laoufi *et al*. (2015)	0.26729	-0.77772	0.18167	0.79866
			TSDT	0.26774	-0.71656	0.18286	0.84003
			SSDT	0.26775	-0.71694	0.18298	0.86748

The computed results using the present HSDT are compared with those reported by other higher-order shear deformation theories as is indicated in Tables 5 and 6.

An excellent agreement between the presented results is confirmed thought this study. These examples show also the influences of the gradient index k and elastic foundation on the non-dimensional deflection and stresses of FG plate, It is important to see that the stresses for a fully ceramic plate are not the same as that for a fully metal plate with elastic foundations. This is because the plate here is affected with the introduction of the temperature field. The number of primary unknowns in this model is even less than that of other HSDTs.

It can be concluded that the present theory is not only accurate but also comparatively simple and quite elegant in predicting the hygro-thermo-mechanical bending behavior of FG plates resting on elastic foundations.

Table 6 Effect of side to thickness ratio and elastic foundation parameters on the dimensionless deflection of an FG square plate (q_0=100, $t1$=0, $t2$=$t3$=10, $c1$=0, $c2$=$c3$=100)

p	k_w	k_p	a/h			
			5	10	20	50
Ceramic	0	0	4.0497	1.206	0.494059	0.294638
	100	0	3.07714	0.948305	0.391973	0.23435
	0	100	0.559442	0.189501	0.0804538	0.0484757
	100	100	0.536037	0.18174	0.0771806	0.0465072
1	0	0	5.3187	1.58389	0.648419	0.386365
	100	0	3.76592	1.1683	0.483434	0.288933
	0	100	0.581976	0.197448	0.0838112	0.0504632
	100	100	0.556854	0.189065	0.0802706	0.0483342
2	0	0	5.58968	1.66861	0.685656	0.410235
	100	0	3.87378	1.20963	0.502976	0.301946
	0	100	0.573678	0.196544	0.08393	0.0507766
	100	100	0.548733	0.188137	0.0803575	0.0486187
3	0	0	5.72589	1.71031	0.703206	0.420981
	100	0	3.92709	1.23013	0.512163	0.307702
	0	100	0.570219	0.196474	0.0840838	0.0509238
	100	100	0.545342	0.188043	0.0804938	0.0487525
4	0	0	5.82242	1.73958	0.715375	0.428339
	100	0	3.96619	1.24461	0.518504	0.311605
	0	100	0.568694	0.196565	0.0842131	0.0510253
	100	100	0.543835	0.188111	0.0806106	0.0488454
5	0	0	5.89976	1.76305	0.725206	0.434346
	100	0	3.99829	1.25615	0.523574	0.314763
	0	100	0.567978	0.567978	0.0843094	0.0511038
	100	100	0.543114	0.188178	0.0806969	0.0489171
Metal	0	0	6.82003	2.04726	0.85215	0.517368
	100	0	4.37574	1.38303	0.583543	0.355662
	0	100	0.567094	0.195342	0.0844888	0.051868
	100	100	0.541922	0.186784	0.0808012	0.0496067

Figs. 2 and 3 present the variation of the non-dimensional center deflection $\overline{w}$ versus the side-to-thickness thickness a/h and plate aspect ratios a/b respectively. It can be seen that the deflection is maximum for the fully metallic plate and becomes minimum for the ceramic plate irrespective of the values of temperature, moisture, and elastic foundation coefficient.

It is evident that for the FG plates the values of the deflections are between those of fully metallic and fully ceramic plates. In addition, the deflection is increased with the absence of the elastic foundation and the influence of moisture load may be less than that of the temperature one.

Figs. 4 to 6 present the through-the-thickness variations of the non-dimensional axial stress $\overline{\sigma}_x$, longitudinal shear stress $\overline{\tau}_{xy}$ and transversal shear stress $\overline{\tau}_{xz}$ in the rectangular FG plates on elastic foundations for different values of moistures and temperatures, respectively. In this figures, it is considered, that $q_0 = 100$ GPa, $a/h = 10$, $b/a = 3$, $p = 2$. As is shown in Figs. 4 and 5, the maximum compressive stresses is found at a point on the top surface and the maximum tensile stresses occur, of course, at a point on the lower surface of the FG plates. It can be observed that the shear stresses increase with the increase of both thermal and moisture load, and the maximum value is found at a point above the mid-plane of the FG plate.

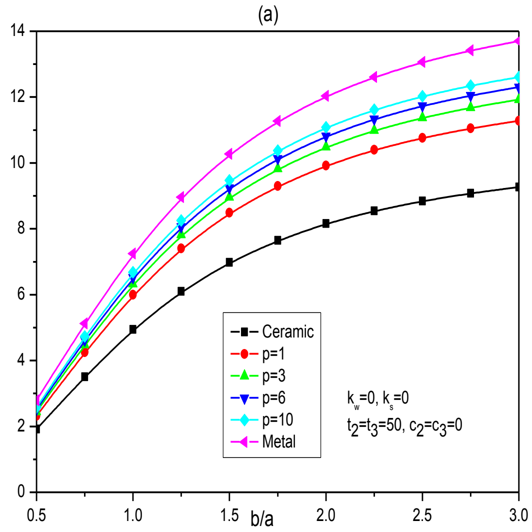

(a)
Ceramic
p=1
p=3
p=6
p=10
Metal
k_w=0, k_s=0
t_2=t_3=50, c_2=c_3=0
b/a

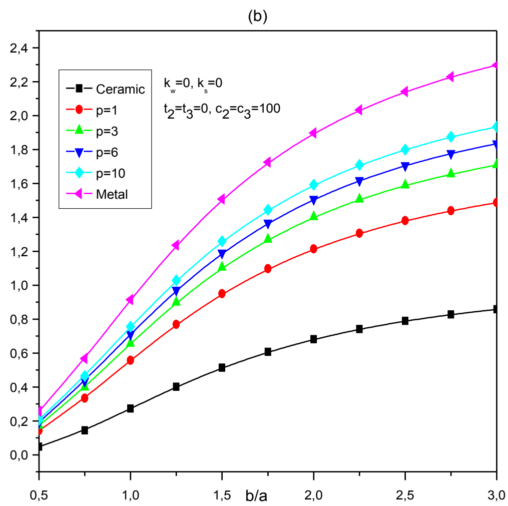

(b)
Ceramic
p=1
p=3
p=6
p=10
Metal
k_w=0, k_s=0
t_2=t_3=0, c_2=c_3=100
b/a

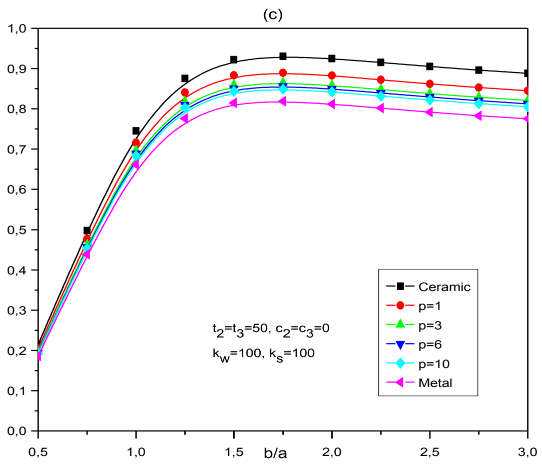

(c)
t_2=t_3=50, c_2=c_3=0
k_w=100, k_s=100
Ceramic
p=1
p=3
p=6
p=10
Metal
b/a

Continued-

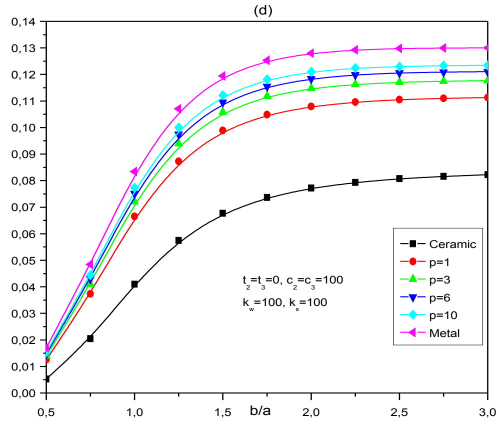

Fig. 2 Non-dimensional center deflection $\bar{w}$ versus plate aspect ratio b/a for FG plate resting on Winkler Pasternak foundations $(a/h=10)$

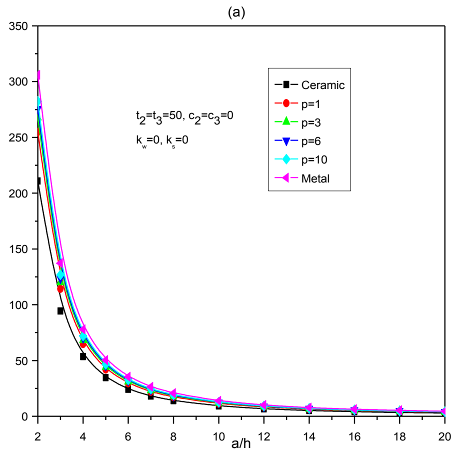

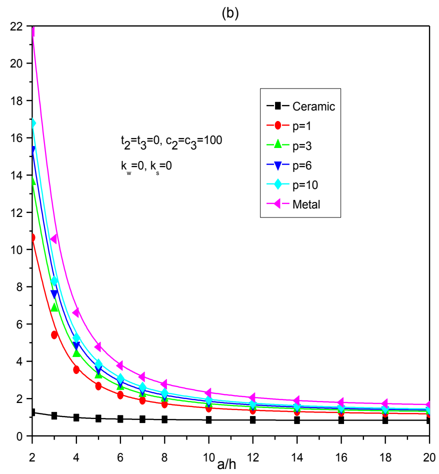

Continued-

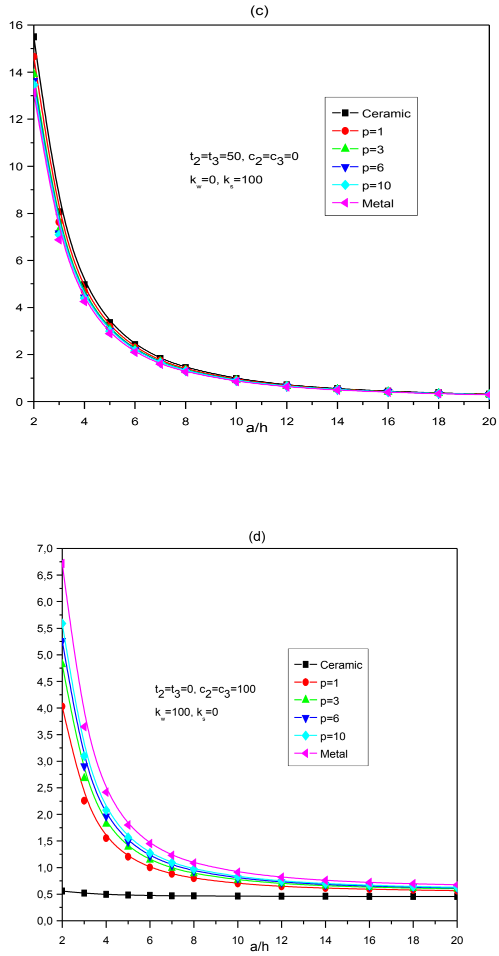

Fig. 3 Non-dimensional center deflection $\overline{w}$ versus side-to-thickness ratio a/h for FG plate on Winkler-Pasternak foundations $\left(b/a=3\right)$

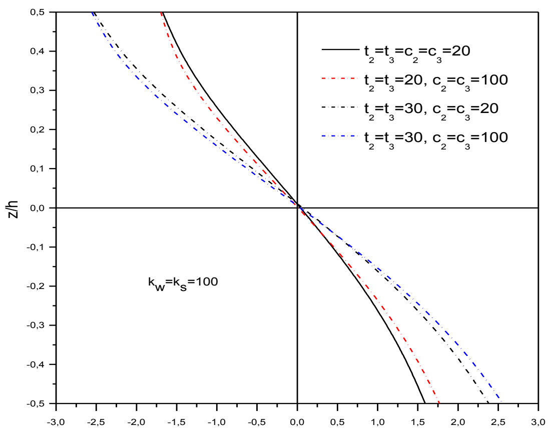

Fig. 4 Variation of non-dimensional axial stress $\overline{\sigma}_x$ through the thickness of a rectangu- lar FG plate on elastic foundations for different values of moistures and temperatures $\left(a/h=10, b/a=3, p=2\right)$

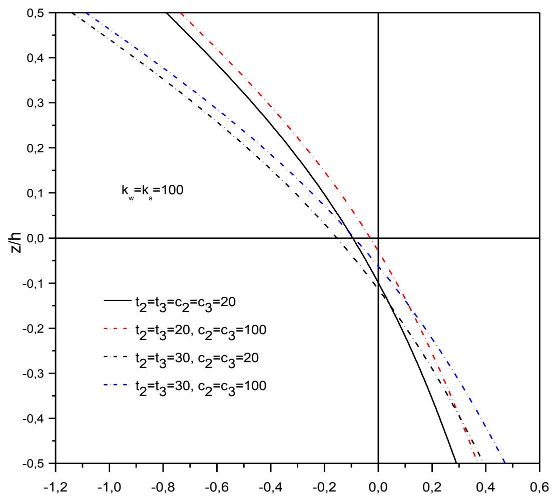

Fig. 5 Variation of non-dimensional in-plane shear stress $\bar{\tau}_{xy}$ through the thickness of a rectangular FG plate on elastic foundations for different values of moistures and temperatures $(a/h=10, b/a=3, p=2)$. $(a/h=10, b/a=3, p=2)$

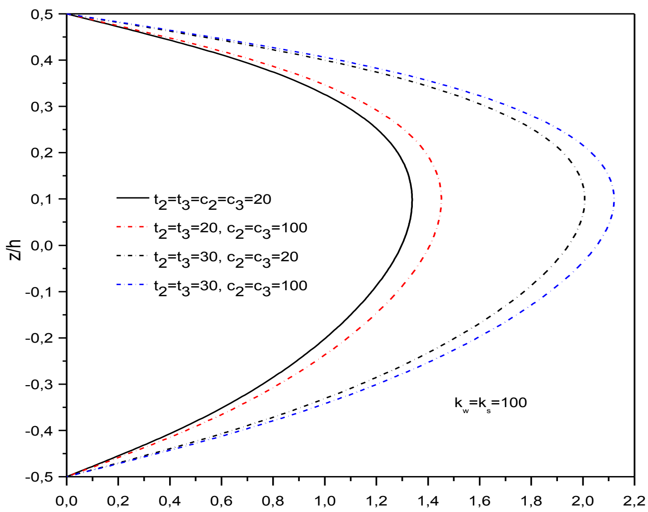

Fig. 6 Variation of non-dimensional transversal shear stress $\bar{\tau}_{xz}$ through the thickness of a rectangular FG plate on elastic foundations for different values of moistures and temperatures $(a/h=10, b/a=3, p=2)$

Figs. 7 to 10 demonstrate the relation between the non-dimensional center deflection $\bar{w}$,the axial stress $\bar{\sigma}_x$ the longitudinal shear stress $\bar{\tau}_{xy}$, the transversal shear stress $\bar{\tau}_{xz}$ and the plate aspect ratio b/a for three different thermal and moisture loading. It's can be seen from these that the three considered cases of temperature and moisture give almost the same values of the non-dimensional center deflection $\bar{w}$, the axial stress $\bar{\sigma}_x$, the longitudinal shear stress $\bar{\tau}_{xy}$ and the transversal shear stress $\bar{\tau}_{xz}$.

Furthermore, the sinusoidal variation provides medium value in deflection and stresses case. The cubic variation gives higher values relatively than those of the other two distributions.

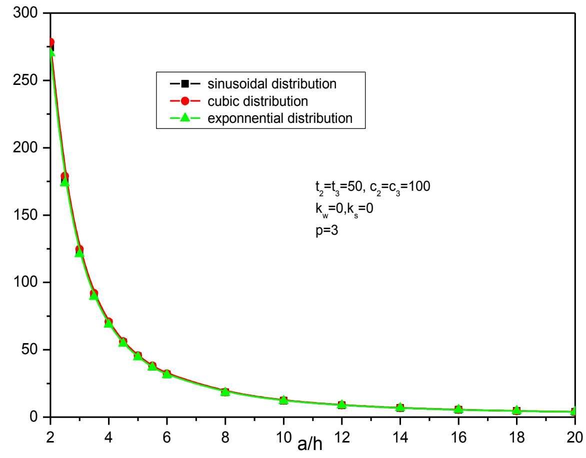

Fig. 7 Dimensionless center deflection $\bar{w}$ versus side-to-thickness ratio a/h for FG plate for different distributions of $\overline{\Psi}(z)$ $(b/a=3, p=2)$

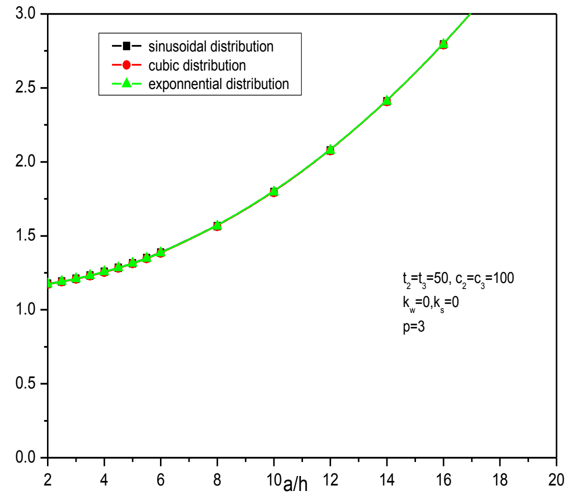

Fig. 8 Dimensionless axial stress $\bar{\sigma}_x$ versus side-to-thickness ratio a/h for FG plate for different distributions of $\overline{\Psi}(z)$ $(b/a=3, p=2)$

The variations of the non-dimensional center deflection $\bar{w}$, the in-plane shear stress $\bar{\tau}_{xy}$, the transversal shear stress $\bar{\tau}_{xz}$ versus the plate aspect ratio b/a for different values of E_m/E_c with or without hygrothermal influences are presented in Figs. 11 to 18. The deflection, the axial and the transversal shear stress increase with increasing the plate aspect ratio b/a, and this quantities take maximum values for $E_m/E_c=0.03$ and minimum ones for $E_m/E_c=1$ as demonstrated in Figs. 11, 12, 14 to 16 and 18.

It can be seen that when hygrothermal effects are not considered, the in-plane shear stress increases with increasing the aspect ratio for b/a less than 1.75. However, when b/a is greater than 1.75 the in-plane shear stress decreases upon increasing the aspect ratio as shown in Fig. 13. In the case where the hygrothermal effects are considered, it can be observed that the in-plane shear stress increases with increasing the aspect ratio for b/a less than 1.0.

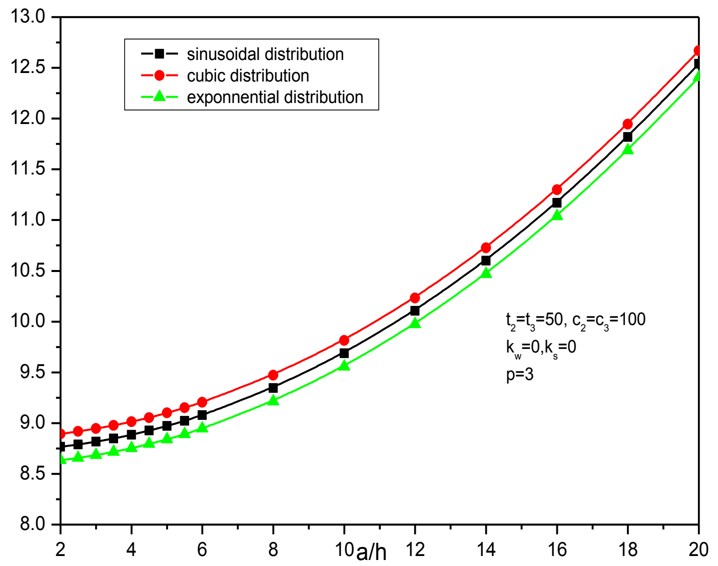

Fig. 9 Dimensionless in-plane shear stress $\bar{\tau}_{xy}$ versus side-to-thickness ratio a/h for FG plate for different distributions of $\overline{\Psi}(z)$ $(b/a=3, p=2)$

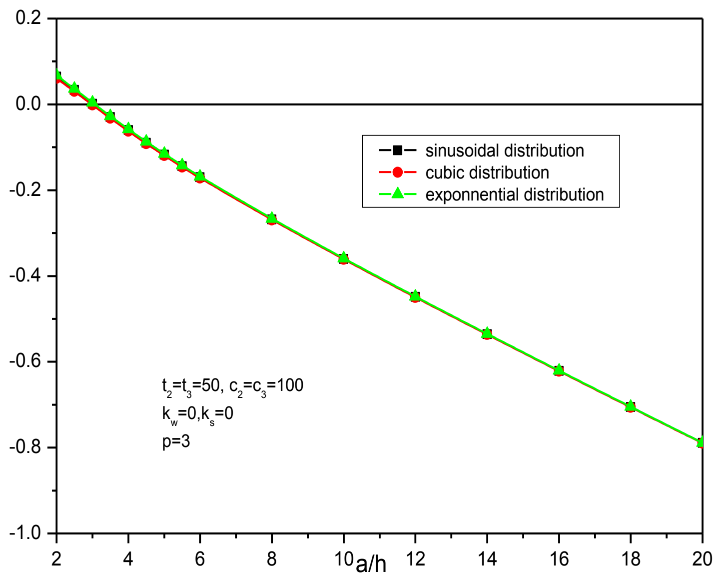

Fig. 10 Dimensionless transversal shear stress $\bar{\tau}_{xz}$ versus side-to-thickness ratio a/h for FG plate for different distributions of $\overline{\Psi}(z)$ $(b/a=3, p=2)$.

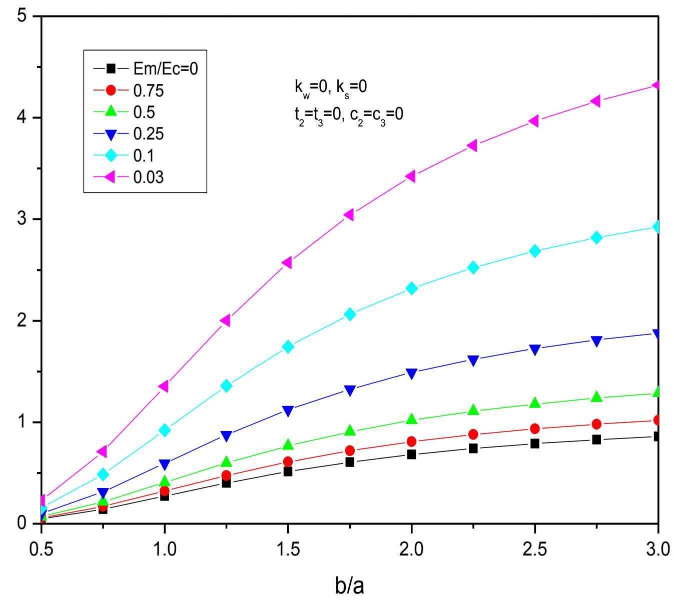

Fig. 11 Dimensionless center deflection $\bar{w}$ versus plate aspect ratio b/a for FG plate for different E_m/E_c ratios $(a/h=10, p=2)$

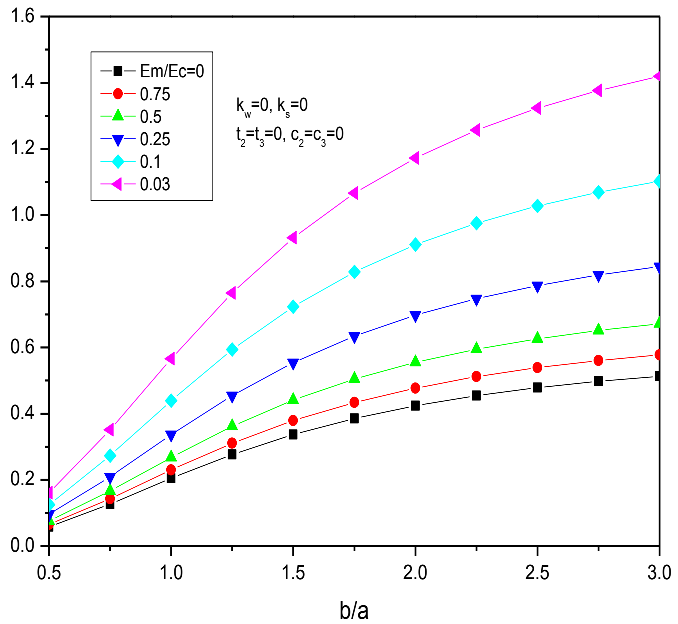

Fig 12 Dimensionless axial stress $\bar{\sigma}_x$ versus plate aspect ratio b/a for FG plate for different E_m/E_c ratios $(a/h=10, p=2)$

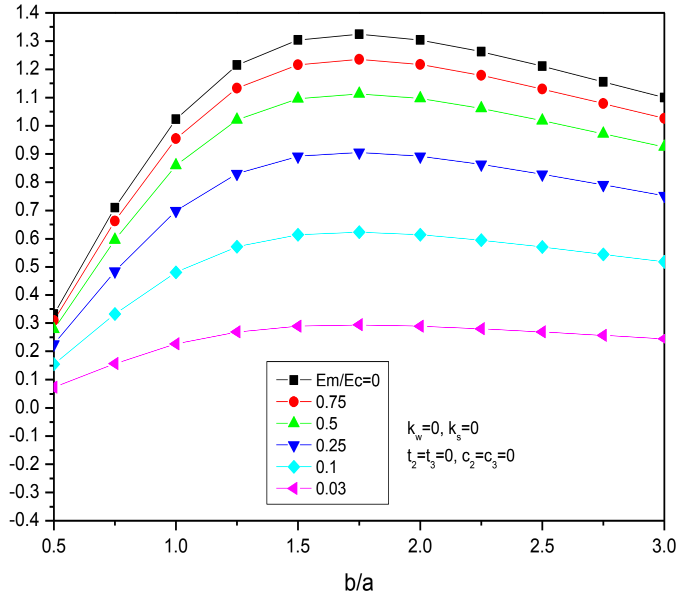

Fig. 13 Dimensionless longitudinal tangential stress $\bar{\tau}_{xy}$ versus plate aspect ratio b/a for FG plate for different E_m/E_c ratios $(a/h=10, p=2)$

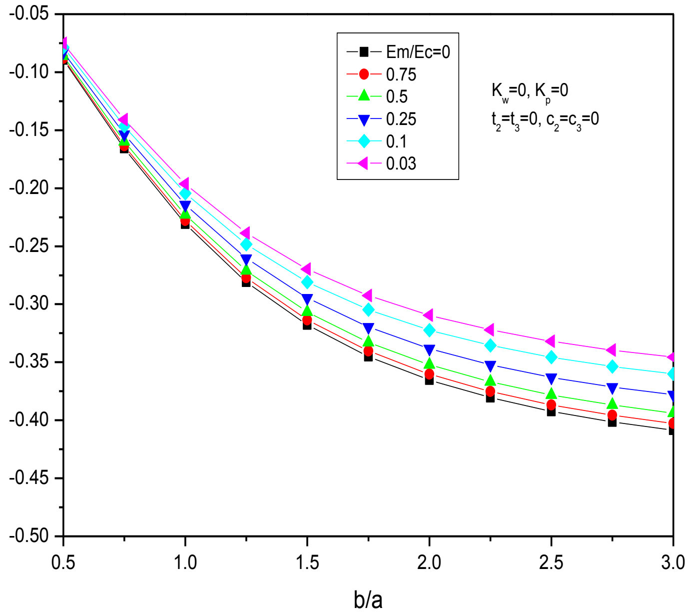

Fig. 14 Dimensionless transversal shear stress $\bar{\tau}_{xz}$ versus plate aspect ratio b/a for FG plate for different E_m/E_c ratios $(a/h=10, p=2)$

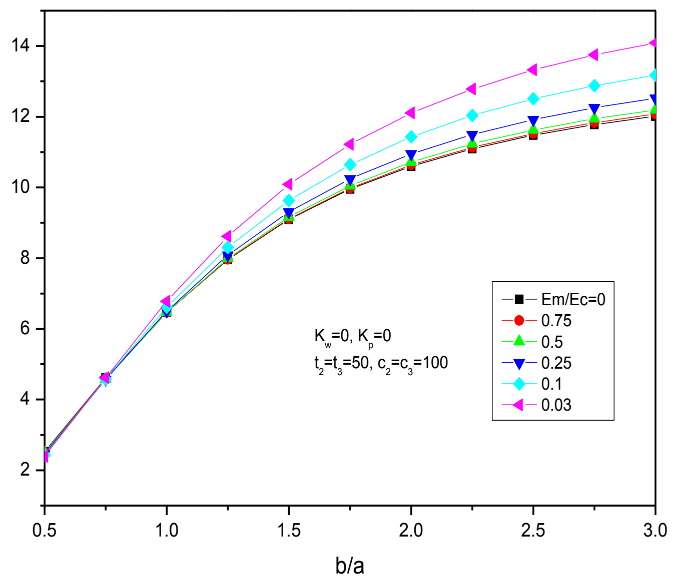

Fig. 15 Dimensionless center deflection $\bar{w}$ versus plate aspect ratio b/a for FG plate for different E_m/E_c ratios $(a/h=10, p=2)$

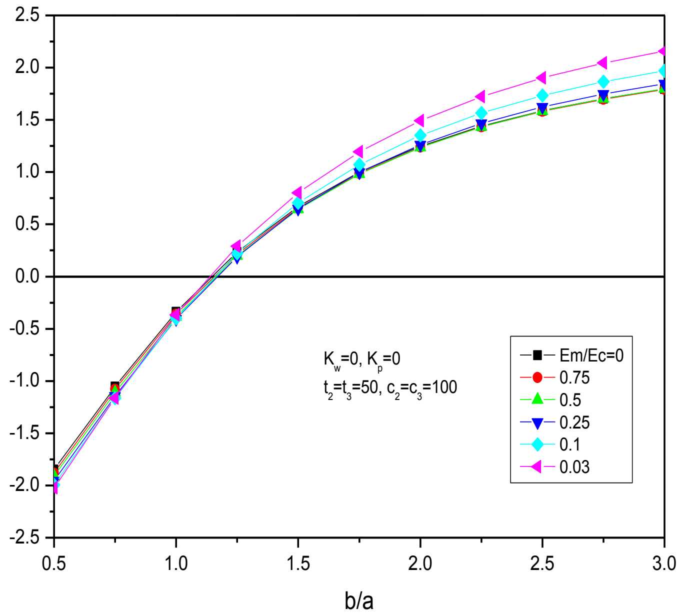

Fig. 16 Dimensionless axial stress $\bar{\sigma}_x$ versus plate aspect ratio b/a for FG plate for different E_m/E_c ratios $(a/h=10, p=2)$

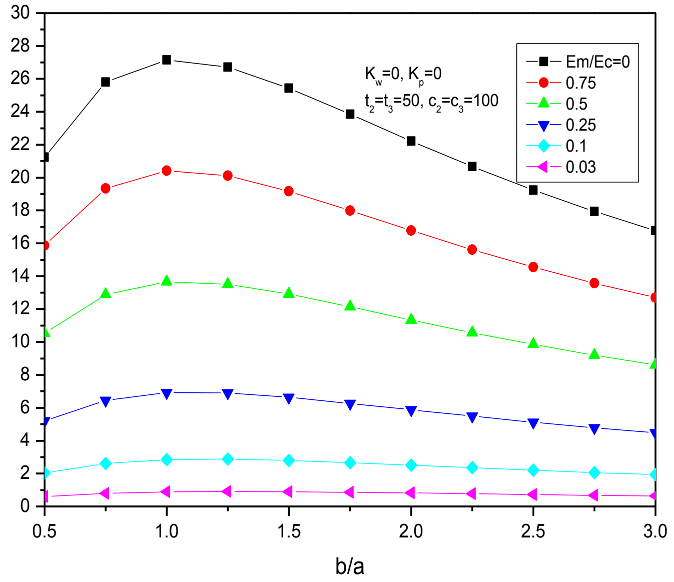

Fig. 17 Dimensionless longitudinal tangential stress $\bar{\tau}_{xy}$ versus plate aspect ratio b/a for FG plate for different E_m/E_c ratios $(a/h=10, p=2)$

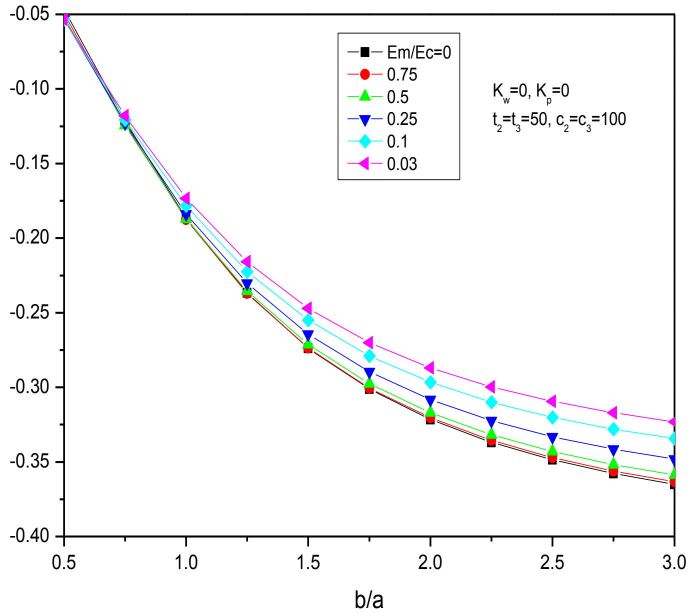

Fig. 18 Dimensionless transversal shear stress $\bar{\tau}_{xz}$ versus plate aspect ratio b/a for FG plate for different E_m/E_c ratios $(a/h=10, p=2)$

However, when b/a is greater than 1.0 the in-plane shear stress is reduced with increasing the aspect ratio. For the two cases with or without considering the hygrothermal effects, the in-plane shear stress is maximum for $E_m/E_c = 1$ and minimum for $E_m/E_c = 0.03$ as shown in Figs. 13 and 17.

5. Conclusions

This article presents the hygro-thermo-mechanical analysis for FG plates using a novel and original HSDT with 4 unknowns. The governing equations are determined through the virtual work's principle. These equations are solved via Navier's method. The results were compared with the solutions of several theories. Illustrating examples are presented to demonstrate the effects of moisture concentration parameter on thermo-mechanical behavior of the FG plates. The good comparisons among the proposed theoretical model, and the other analytical solutions available in the literature, demonstrate that the presented solution can accurately predict the hygro-thermo-mechanical behavior of the FG plate and be employed in the design of the solar plate.

References

Abdelaziz, H.H., Ait Amar Meziane, M., Bousahla, A.A., Tounsi, A., Mahmoud, S.R. and Alwabli, A.S. (2017), "An efficient hyperbolic shear deformation theory for bending, buckling and free vibration of FGM sandwich plates with various boundary conditions", *Steel Compos. Struct.*, **25**(6), 693-704.

Abualnour, M., Houari, M.S.A., Tounsi, A., Adda Bedia, E.A. and Mahmoud, S.R. (2018), "A novel quasi-3D trigonometric plate theory for free vibration analysis of advanced composite plates", *Compos. Struct.*, **184**, 688-697.

Ahmed, A. (2014), "Post buckling analysis of sandwich beams with functionally graded faces using a consistent higher order theory", *Int. J. Civil, Struct. Environ.*, **4**(2), 59-64.

Ahouel, M., Houari, M.S.A., Adda Bedia, E.A. and Tounsi, A. (2016), "Size-dependent mechanical behavior of functionally graded trigonometric shear deformable nanobeams including neutral surface position concept", *Steel Compos. Struct.*, **20**(5), 963-981.

Ait Amar Meziane, M., Abdelaziz, H.H. and Tounsi, A. (2014), "An efficient and simple refined theory for buckling and free vibration of exponentially graded sandwich plates under various boundary conditions", *J. Sandw. Struct. Mater.*, **16**(3), 293-318.

Ait Yahia, S., Ait Atmane, H., Houari, M.S.A. and Tounsi, A. (2015), "Wave propagation in functionally graded plates with porosities using various higher-order shear deformation plate theories", *Struct. Eng. Mech.*, **53**(6), 1143-1165.

Akavci, S.S. (2015), "An efficient shear deformation theory for free vibration of functionally graded thick rectangular plates on elastic foundation", *Compos. Struct.*, **108**, 667-676.

Akbaş, Ş.D. (2015), "Wave propagation of a functionally graded beam in thermal environments", *Steel Compos. Struct.*, **19**(6), 1421-1447.

Al-Basyouni, K.S., Tounsi, A. and Mahmoud, S.R. (2015), "Size dependent bending and vibration analysis of functionally graded micro beams based on modified couple stress theory and neutral surface position", *Compos. Struct.*, **125**, 621-630.

Aldousari, S.M. (2017), "Bending analysis of different material distributions of functionally graded beam", *Appl. Phys. A: Mater. Sci. Process.*, **123**(4), 296.

Attia, A., Tounsi, A., Adda Bedia, E.A. and Mahmoud, S.R. (2015), "Free vibration analysis of functionally graded plates with temperature-dependent properties using various four variable refined plate theories", *Steel Compos. Struct.*, **18**(1), 187-212.

Barati, M.R. and Shahverdi, H. (2016), "A four-variable plate theory for thermal vibration of embedded FG nanoplates under non-uniform temperature distributions with different boundary conditions", *Struct. Eng. Mech.*, **60**(4), 707-727.

Barka, M., Benrahou, K.H., Bakora, A. and Tounsi, A. (2016), "Thermal post-buckling behavior of imperfect temperature-dependent sandwich FGM plates resting on Pasternak elastic foundation", *Steel Compos. Struct.*, **22**(1), 91-112.

Belabed, Z., Houari, M.S.A., Tounsi, A., Mahmoud, S.R. and Anwar Bég, O. (2014), "An efficient and simple higher order shear and normal deformation theory for functionally graded material (FGM) plates", *Compos. : Part B*, **60**, 274-283.

Beldjelili, Y., Tounsi, A. and Mahmoud, S.R. (2016), "Hygro-thermo-mechanical bending of S-FGM plates resting on variable elastic foundations using a four-variable trigonometric plate theory", *Smart Struct. Syst.*, **18**(4), 755-786.

Belkorissat, I., Houari, M.S.A., Tounsi, A., Adda Bedia, E.A. and Mahmoud, S.R. (2015), "On vibration properties of functionally graded nano-plate using a new nonlocal refined four variable model", *Steel Compos. Struct.*, **18**(4), 1063-1081.

Bellifa, H., Bakora, A., Tounsi, A., Bousahla, A.A. and Mahmoud, S.R. (2017b), "An efficient and simple four variable refined plate theory for buckling analysis of functionally graded plates", *Steel Compos. Struct.*, **25**(3), 257-270.

Bellifa, H., Benrahou, K.H., Bousahla, A.A., Tounsi, A. and Mahmoud, S.R. (2017a), "A nonlocal zeroth-order shear deformation theory for nonlinear postbuckling of nanobeams", *Struct. Eng. Mech.*, **62**(6), 695 - 702.

Bellifa, H., Benrahou, K.H., Hadji, L., Houari, M.S.A. and Tounsi, A. (2016), "Bending and free vibration analysis of functionally graded plates using a simple shear deformation theory and the concept the neutral surface position", *J. Braz. Soc. Mech. Sci. Eng.*, **38**, 265-275.

Benadouda, M., Ait Atmane, H., Tounsi, A., Bernard, F. and Mahmoud, S.R. (2017), "An efficient shear deformation theory for wave propagation in functionally graded material beams with porosities", *Earthq. Struct.*, **13**(3), 255-265.

Benchohra, M., Driz, H., Bakora, A., Tounsi, A., Adda Bedia, E.A. and Mahmoud, S.R. (2018), "A new quasi-3D sinusoidal shear deformation theory for functionally graded plates", *Struct. Eng. Mech.*, (In press).

Bennoun, M., Houari, M.S.A. and Tounsi, A. (2016), "A novel five variable refined plate theory for vibration analysis of functionally graded sandwich plates", *Mech. Adv. Mater. Struct.*, **23**(4), 423-431.

Bessaim, A., Houari, M.S.A., Tounsi, A., Mahmoud, S.R. and Adda Bedia, E.A. (2013), "A new higher order shear and normal deformation theory for the static and free vibration analysis of sandwich plates with functionally graded isotropic face sheets", *J. Sandw. Struct.Mater.*, **15**, 671-703.

Besseghier, A., Houari, M.S.A., Tounsi, A. and Mahmoud, S.R. (2017), "Free vibration analysis of embedded nanosize FG plates using a new nonlocal trigonometric shear deformation theory", *Smart Struct. Syst.*, **19**(6), 601-614.

Bouafia, K., Kaci, A., Houari, M.S.A., Benzair, A. and Tounsi, A. (2017), "A nonlocal quasi-3D theory for bending and free flexural vibration behaviors of functionally graded nanobeams", *Smart Struct. Syst.*, **19**(2), 115-126.

Bouderba, B., Houari, M.S.A. and Tounsi, A. (2013), “Thermomechanical bending response of FGM thick plates resting on Winkler-Pasternak elastic foundations”, *Steel Compos. Struct.*, **14**(1), 85-104.

Bouderba, B., Houari, M.S.A. and Tounsi, A. and Mahmoud, S.R. (2016), “Thermal stability of functionally graded sandwich plates using a simple shear deformation theory”, *Struct. Eng. Mech*., **58**(3), 397-422.

Boukhari, A., Ait Atmane, H., Tounsi, A., Adda Bedia, E.A. and Mahmoud, S.R. (2016), “An efficient shear deformation theory for wave propagation of functionally graded material plates”, *Struct. Eng. Mech*., **57**(5), 837-859.

Bounouara, F., Benrahou, K.H., Belkorissat, I. and Tounsi, A. (2016), “A nonlocal zeroth-order shear deformation theory for free vibration of functionally graded nanoscale plates resting on elastic foundation”, *Steel Compos. Struct.*, **20**(2), 227-249.

Bourada, M., Kaci, A., Houari, M.S.A. and Tounsi, A. (2015), “Anew simple shear and normal deformations theory for functionally graded beams”, *Steel Compos. Struct*., **18**(2), 409-423.

Bousahla, A.A., Attia, A., Tounsi, A., Mahmoud, S.R. and Alwabli, A.S. (2018), “A refined four variable plate theory for thermoelastic analysis of FGM plates resting on variable elastic foundations”, *Struct. Eng. Mech*., (In press).

Bousahla, A.A., Benyoucef, S., Tounsi, A., Mahmoud, S.R. (2016), “On thermal stability of plates with functionally graded coefficient of thermal expansion”, *Struct. Eng. Mech*., **60**(2), 313-335.

Bousahla, A.A., Houari, M.S.A., Tounsi, A. and Adda Bedia, E.A. (2014), “A novel higher order shear and normal deformation theory based on neutral surface position for bending analysis of advanced composite plates”, *Int. J. Comput. Meth*., **11**(6), 1350082.

Chikh, A., Tounsi, A., Hebali, H. and Mahmoud, S.R. (2017), “Thermal buckling analysis of cross-ply laminated plates using a simplified HSDT”, *Smart Struct. Syst*., **19**(3), 289-297.

Darılmaz, K. (2015), “Vibration analysis of functionally graded material (FGM) grid systems”, *Steel Compos*. *Struct*., **18**(2), 395-408.

Draiche, K., Tounsi, A. and Mahmoud, S.R. (2016), “A refined theory with stretching effect for the flexure analysis of laminated composite plates”, *Geomech. Eng.*, **11**(5), 671-690.

El Haina, F., Bakora, A., Bousahla, A.A., Tounsi, A. and Mahmoud, S.R. (2017), “A simple analytical approach for thermal buckling of thick functionally graded sandwich plates”, *Struct. Eng. Mech*., **63**(5), 585-595.

Fallah, F. and Nosier, A. (2012), “Nonlinear behavior of functionally graded circular plates with various boundary supports under asymmetric thermo-mechanical loading”, *Compos. Struct.*, **94**(9), 2834-2850.

Golmakani, M.E. and Kadkhodayan, M. (2011), “Large deflection analysis of circular and annular FGM plates under thermo-mechanical loadings with temperature dependent properties”, *Compos. :Part B,* **42**(4), 614 - 625.

Hadji, L. and Adda Bedia, E.A. (2015), “Analyse of the behavior of functionally graded beams based on neutral surface position”, *Struct*. *Eng*. *Mech*., **55**(4), 703-717.

Hamidi, A., Houari, M.S.A., Mahmoud, S.R. and Tounsi, A. (2015), “A sinusoidal plate theory with 5-unknowns and stretching effect for thermomechanical bending of functionally graded sandwich plates”, *Steel Compos. Struct*., **18**(1), 235-253.

Hanifi Hachemi Amar, L., Kaci, A. and Tounsi, A. (2017), “On the size-dependent behavior of functionally graded micro-beams with porosities”, *Struct. Eng. Mech.*, **64**(5), 527-541.

Hebali, H., Tounsi, A., Houari, M.S.A., Bessaim, A. and Adda Bedia, E.A. (2014), “A new quasi-3D hyperbolic shear deformation theory for the static and free vibration analysis of functionally graded plates”, *J. Eng. Mech. - ASCE*, **140**(2), 374-383.

Hirwani, C.K., Panda, S.K., Mahapatra, T.R. and Mahapatra, S.S. (2017), “Nonlinear transient finite-element analysis of delaminated composite shallow shell panels”, *AIAA J.*, **55**(5), 1734-1748.

Hirwani, C.K., Panda, S.P., Mahapatra, S.S., Mandal, S.K., Srivastava, L. and Buragohain, S.K. (2016), “Flexural strength of delaminated composite plate – An experimental validation”, *Int. J. Damage Mech.*, (In press).

Hirwani, C.K., Panda, S.P. and Mahapatra, T.R. (2018a), “Thermomechanical deflection and stress responses of delaminated shallow shell structure using higher-order theories”, *Compos. Struct.*, **184**, 135-145.

Hirwani, C.K., Panda, S.P., Mahapatra, T.R., Mandal, S.K., Mahapatra, S.S. and De, A.K. (2018b), “Delamination effect on flexural responses of layered curved shallow shell panel-experimental and numerical analysis”, *Int. J. Comput.Meth.*, **15**(1), 1850027.

Houari, M.S.A., Tounsi, A., Bessaim, A. and Mahmoud, S.R. (2016), “A new simple three- unknown sinusoidal shear deformation theory for functionally graded plates”, *Steel Compos. Struct*., **22**(2), 257-276.

Houari, M.S.A., Tounsi, A. and Bég, O.A. (2013), “Thermoelastic bending analysis of functionally graded sandwich plates using a new higher order shear and normal deformation theory”, *Int. J. Mech. Sci.*, **76**(6), 102-111.

Kar, V.R. and Panda, S.K. (2015a), “Nonlinear flexural vibration of shear deformable functionally graded spherical shell panel”, *Steel Compos*. *Struct*., **18**(3), 693-709.

Kar, V.R. and Panda, S.K. (2015b), “Thermoelastic analysis of functionally graded doubly curved shell panels using nonlinear finite element method”, *Compos. Struct.*, **129**, 202-212.

Kar, V.R. and Panda, S.K. (2015c), “Large deformation bending analysis of functionally graded spherical shell using FEM”, *Struct. Eng. Mech.*, **53**(4), 661-679.

Kar, V.R. and Panda, S.K. (2016a), “Nonlinear thermo-mechanical behaviour of FGM cylindrical/hyperbolic/elliptical shell panel with TD and TID properties”, *J. Press. Vess. – T. ASME*, **138**(6), 6-13.

Kar, V.R. and Panda, S.K. (2016b), “Nonlinear thermomechanical deformation behaviour of P-FGM shallow spherical shell panel”, *Chinese J. Aeronaut.*, **29**(1), 173-183.

Kar, V.R. and Panda, S.K. (2016c), “Nonlinear free vibration of functionally graded doubly curved shear deformable panels using finite element method”, *J. Vib. Control*, **22**(7), 1935-1949.

Kar, V.R., Mahapatra, T.R. and Panda, S.K. (2015), “Nonlinear flexural analysis of laminated composite flat panel under hygro-thermo-mechanical loading”, *Steel Compos*. *Struct*., **19**(4), 1011-1033.

Khetir, H., Bachir Bouiadjra, M., Houari, M.S.A., Tounsi, A., and Mahmoud, S.R. (2017), “A new nonlocal trigonometric shear deformation theory for thermal buckling analysis of embedded nanosize FG plates”, *Struct. Eng. Mech.*, **64**(4), 391-402.

Kolahchi, R., Safari, M. and Esmailpour, M. (2016), “Dynamic stability analysis of temperature-dependent functionally graded CNT-reinforced visco-plates resting on orthotropic elastomeric medium”, *Compos. Struct.*, **150**, 255- 265.

Laoufi, I., Ameur, M., Zidi, M., Adda Bedia, E.A. and Bousahla, A.A. (2016), “Mechanical and hygrothermal behaviour of functionally graded plates using a hyperbolic shear deformation theory”, *Steel Compos. Struct.*, **20**(4), 889-911.

Larbi Chaht, F., Kaci, A., Houari, M.S.A., Tounsi, A., Anwar Bég, O. and Mahmoud, S.R. (2015), “Bending and buckling analyses of functionally graded material (FGM) size-dependent nanoscale beams including the thickness stretching effect”, *Steel Compos. Struct.*, **18**(2), 425-442.

Li, D., Deng, Z. and Xiao, H. (2016), "Thermomechanical bending analysis of functionally graded sandwich plates using four-variable refined plate theory", *Compos.: Part B*, **106**, 107-119.

Liew, K.M., Kitipornchai, S., Zhang, X.Z. and Lim, C.W. (2003), "Analysis of the thermal stress behaviour of functionally graded hollow circular cylinders", *Int. J. Solids Struct.*, **40**, 2355-2380.

Mahapatra, T.R., Kar, V.R., Panda, S.K. and Mehar, K. (2017), "Nonlinear thermoelastic deflection of temperature-dependent FGM curved shallow shell under nonlinear thermal loading", *J. Therm. Stresses*, **40**(9), 1184-1199.

Mahapatra, T.R., Panda, S.K. and Kar, V.R. (2016a), "Geometrically nonlinear flexural analysis of hygro-thermo-elastic laminated composite doubly curved shell panel", *Int. J. Mech. Mater. Des*., **12**(2), 153-171.

Mahapatra, T.R., Panda, S.K. and Kar, V.R. (2016b), "Nonlinear flexural analysis of laminated composite panel under hygro-thermo-mechanical loading -a micromechanical approach", *Int. J. Comput.Meth.*, **13**(3), 1650015.

Mahi, A., Adda Bedia, E.A. and Tounsi, A. (2015), "A new hyperbolic shear deformation theory for bending and free vibration analysis of isotropic, functionally graded, sandwich and laminated composite plates", *Appl. Math. Model*., **39**(9), 2489-2508.

Mantari, JL, Granados, EV. (2015), "Thermoelastic analysis of advanced sandwich plates based on a new quasi-3D hybrid type HSDT with 5 unknowns", *Composites Part B*, **69**, 317 - 334.

Mehar, K. and Panda, S.K. (2017), "Numerical investigation of nonlinear thermomechanical deflection of functionally graded CNT reinforced doubly curved composite shell panel under different mechanical loads", *Compos. Struct.*, **161**, 287-298.

Menasria, A., Bouhadra, A., Tounsi, A., Bousahla, A.A. and Mahmoud, S.R. (2017), "A new and simple HSDT for thermal stability analysis of FG sandwich plates", *Steel Compos. Struct.*, **25**(2), 157-175.

Mouffoki, A., Adda Bedia, E.A., Houari, M.S.A., Tounsi, A. and Mahmoud, S.R. (2017), "Vibration analysis of nonlocal advanced nanobeams in hygro-thermal environment using a new two-unknown trigonometric shear deformation beam theory", *Smart Struct. Syst*., **20**(3), 369-383.

Rahmani, O., Refaeinejad, V. and Hosseini, S.A.H. (2017), "Assessment of various nonlocal higher order theories for the bending and buckling behavior of functionally graded nanobeams", *Steel Compos. Struct.*, **23**(3), 339-350.

Reddy, J.N. (2000), "Analysis of functionally graded plates", *Int. J. Numer. Meth. Eng*., **47**(1-3), 663-684.

Reddy, J.N. (2011), "A general nonlinear third-order theory of functionally graded plates", *Int. J. Aerosp. Lightweight Struct.*, **1**(1), 1-21.

Reddy, J.N. and Cheng, Z.Q. (2001), "Three-dimensional thermomechanical deformations of functionally graded rectangular plates", *Eur. J. Mech. A-Solids*, **20**, 841-855.

Saidi, H., Tounsi, A. and Bousahla, A.A. (2016), "A simple hyperbolic shear deformation theory for vibration analysis of thick functionally graded rectangular plates resting on elastic foundations", *Geomech. Eng.*, **11**(2), 289-307.

Shukla, K.K., Kumar, K.V.R., Pandey, R. and Nath, Y. (2007), "Postbuckling response of functionally graded rectangular plates subjected to thermo-mechanical loading", *Int. J. Struct. Stab. Dynam*, **7**(3), 519-541.

Sobhy, M. (2015), "Thermoelastic response of FGM plates with temperature-dependent properties resting on variable elastic foundations", *Int. J. Appl. Mech.*, **7**, 1550082.

Swaminathan, K. and Naveenkumar, D.T. (2014), "Higher order refined computational models for the stability analysis of FGM plates: Analytical solutions", *Eur. J. Mech. A - Solid.*, **47**, 349-361.

Tounsi, A, Houari, M.S.A. and Benyoucef, S. (2013), "A refined trigonometric shear deformation theory for thermoelastic bending of functionally graded sandwich plates", *Aerosp Sci Technol.*, **24**(1), 209-220.

Tung, H.V. and Duc, N.D. (2014), "Nonlinear response of shear deformable FGM curved panels resting on elastic foundations and subjected to mechanical and thermal loading conditions", *Appl. Math Model.*, **38**(11), 2848-6628.

Vel, S.S. and Batra, R.C. (2003), "Three-dimensional analysis of transient thermal stresses in functionally graded plates", *Int. J. Solids Struct.*, **40**, 7181-7196.

Yaghoobi, H. and Yaghoobi, P. (2013), "Buckling analysis of sandwich plates with FGM face sheets resting on elastic foundation with various boundary conditions: an analytical approach", *Meccanica.*, **48**(8), 2019-2035.

Yazid, M., Heireche, H., Tounsi, A., Bousahla, A.A. and Houari, M.S.A. (2018), "A novel nonlocal refined plate theory for stability response of orthotropic single-layer graphene sheet resting on elastic medium", *Smart Struct. Syst*., (Accepted).

Youcef, D.O., Kaci, A., Benzair, A., Bousahla, A.A. and Tounsi, A. (2018), "Dynamic analysis of nanoscale beams including surface stress effects", *Smart Struct. Syst*., (Accepted).

Zaman, M., Yan, Z. and Jiang, L. (2010), "Thermal effect on the bending behavior of curved functionally graded piezoelectric actuators", *Int. J. Appl. Mech*, **2**(4), 787-805.

Zemri, A., Houari, M.S.A., Bousahla, A.A. and Tounsi, A. (2015), "A mechanical response of functionally graded nanoscale beam: an assessment of a refined nonlocal shear deformation theory beam theory", *Struct. Eng. Mech.*, **54**(4), 693-710.

Zenkour, A.M. (2006), "Generalized shear deformation theory for bending analysis of functionally graded plates", *Appl. Math. Model.*, **30**(1), 67-84.

Zhang, X.D., Liu, D.Q. and Ge, C. (1994), "Thermal stress analysis of axial symmetry functionally gradient materials under steady temperature field", *J. Funct. Grad. Mater.*, **25**, 452–455.

Zhu, P., Zhang, L.W. and Liew, K.M. (2014), "Geometrically nonlinear thermomechanical analysis of moderately thick functionally graded plates using a local Petrove Galerkin approach with moving Kriging interpolation", *Compos. Struct.*, **107**, 298-314.

Zidi, M., Houari, M.S.A., Tounsi, A., Bessaim, A. and Mahmoud, S.R. (2017), "A novel simple two-unknown hyperbolic shear deformation theory for functionally graded beams", *Struct. Eng. Mech.*, **64**(2), 145-153.

Zidi, M., Tounsi, A., Houari, M.S.A., Adda Bedia, E.A. and Bég, O.A. (2014), "Bending analysis of FGM plates under hygro-thermo-mechanical loading using a four variable refined plate theory", *Aerosp. Sci. Technol.*, **34**, 24-34.

CC